BJP British Journal of Pharmacology

DOI:10.1111/j.1476-5381.2012.01914.x
www.brjpharmacol.org

RESEARCH PAPER

Inhibitory effects of sevoflurane on pacemaking activity of sinoatrial node cells in guinea-pig heart

Akiko Kojima[1,2], Hirotoshi Kitagawa[1], Mariko Omatsu-Kanbe[2], Hiroshi Matsuura[2] and Shuichi Nosaka[1]

[1]*Department of Anesthesiology, Shiga University of Medical Science, Otsu, Shiga, Japan, and* [2]*Department of Physiology, Shiga University of Medical Science, Otsu, Shiga, Japan*

Correspondence
Akiko Kojima, Department of Anesthesiology, Shiga University of Medical Science, Otsu, Shiga 520-2192, Japan. E-mail: akiko77@belle.shiga-med.ac.jp

Keywords
sevoflurane; sinoatrial node; spontaneous action potential; diastolic depolarization; pacemaker; firing rate; I_f; $I_{Ca,T}$; $I_{Ca,L}$; heart rate

Received
24 August 2011
Revised
17 February 2012
Accepted
18 February 2012

BACKGROUND AND PURPOSE

The volatile anaesthetic sevoflurane affects heart rate in clinical settings. The present study investigated the effect of sevoflurane on sinoatrial (SA) node automaticity and its underlying ionic mechanisms.

EXPERIMENTAL APPROACH

Spontaneous action potentials and four ionic currents fundamental for pacemaking, namely, the hyperpolarization-activated cation current (I_f), T-type and L-type Ca^{2+} currents ($I_{Ca,T}$ and $I_{Ca,L}$, respectively), and slowly activating delayed rectifier K^+ current (I_{Ks}), were recorded in isolated guinea-pig SA node cells using perforated and conventional whole-cell patch-clamp techniques. Heart rate in guinea-pigs was recorded *ex vivo* in Langendorff mode and *in vivo* during sevoflurane inhalation.

KEY RESULTS

In isolated SA node cells, sevoflurane (0.12–0.71 mM) reduced the firing rate of spontaneous action potentials and its electrical basis, diastolic depolarization rate, in a qualitatively similar concentration-dependent manner. Sevoflurane (0.44 mM) reduced spontaneous firing rate by approximately 25% and decreased I_f, $I_{Ca,T}$, $I_{Ca,L}$ and I_{Ks} by 14.4, 31.3, 30.3 and 37.1%, respectively, without significantly affecting voltage dependence of current activation. The negative chronotropic effect of sevoflurane was partly reproduced by a computer simulation of SA node cell electrophysiology. Sevoflurane reduced heart rate in Langendorff-perfused hearts, but not *in vivo* during sevoflurane inhalation in guinea-pigs.

CONCLUSIONS AND IMPLICATIONS

Sevoflurane at clinically relevant concentrations slowed diastolic depolarization and thereby reduced pacemaking activity in SA node cells, at least partly due to its inhibitory effect on I_f, $I_{Ca,T}$ and $I_{Ca,L}$. These findings provide an important electrophysiological basis of alterations in heart rate during sevoflurane anaesthesia in clinical settings.

Abbreviations

APA, action potential amplitude; APD, action potential duration; APD_{50}, action potential duration measured from the peak to 50% repolarization; APD_{90}, action potential duration measured from the peak to 90% repolarization; DDR, diastolic depolarization rate; $g_{Ca,L}$, conductance of L-type Ca^{2+} current; $g_{Ca,T}$, conductance of T-type Ca^{2+} current; g_f, conductance of hyperpolarization-activated cation current; HCN, hyperpolarization-activated cyclic nucleotide-gated channel; I_{Ca}, voltage-dependent Ca^{2+} current; $I_{Ca,L}$, L-type Ca^{2+} current; $I_{Ca,T}$, T-type Ca^{2+} current; I_f, hyperpolarization-activated cation current; I_{Kr}, rapidly activating delayed rectifier K^+ current; I_{Ks}, slowly activating delayed rectifier K^+ current; I_{NCX}, Na^+/Ca^{2+} exchange current; *I-V*, current-voltage; *k*, slope factor; KB, Kraftbrühe; max $dV \cdot dt^{-1}$, maximum upstroke velocity; MDP, maximum diastolic potential; SA, sinoatrial; τ, time constant; $V_{1/2}$, voltage at half-maximal activation

Introduction

The spontaneous activity of the sinoatrial (SA) node underlies the intrinsic automaticity of mammalian heart and is profoundly affected by the autonomic nervous system. The diastolic depolarization (pacemaker depolarization) in SA node action potentials plays an essential role in the generation of spontaneous electrical activity and is due to a very small net inward current produced by a complex but coordinated interaction of several inwardly and outwardly directed ion currents (DiFrancesco, 1993; Dobrzynski *et al.*, 2007; Mangoni and Nargeot, 2008; Verkerk *et al.*, 2009). These include the activation of inward currents such as the hyperpolarization-activated cation current (I_f) (DiFrancesco, 1991), T-type and L-type Ca^{2+} currents ($I_{Ca,T}$ and $I_{Ca,L}$, respectively) (Hagiwara *et al.*, 1988; Verheijck *et al.*, 1999; Mangoni *et al.*, 2003; 2006), background non-selective cation current (Hagiwara *et al.*, 1992) and Ca^{2+} release-activated Na^+/Ca^{2+} exchange current (I_{NCX}; Bogdanov *et al.*, 2006), and deactivation of outward currents such as the rapidly and slowly activating delayed rectifier K^+ currents (I_{Kr} and I_{Ks} respectively) [Verheijck *et al.*, 1995; Ono *et al.*, 2000; Matsuura *et al.*, 2002; channel nomenclature follows Alexander *et al.* (2011)].

Although there is some debate regarding the physiological relevance of I_f in SA node pacemaking, available electrophysiological and pharmacological data indicate that I_f is activated and produces an inward current during diastolic depolarization (especially in its early phase) in various mammalian species including humans (DiFrancesco, 1991; BoSmith *et al.*, 1993; Mangoni and Nargeot, 2001; Thollon *et al.*, 2007; Verkerk *et al.*, 2007; Baruscotti *et al.*, 2010). Molecular genetic and functional studies have also shown that loss-of-function mutations in the gene encoding the hyperpolarization-activated cyclic nucleotide-gated channel 4 (HCN4), the dominant component of human I_f (Shi *et al.*, 1999), are responsible for SA node dysfunction associated with sinus bradycardia (Schulze-Bahr *et al.*, 2003; Ueda *et al.*, 2004; Milanesi *et al.*, 2006; Nof *et al.*, 2007), which provides further evidence that I_f contributes to SA node pacemaker activity in humans.

A number of studies have investigated the effects of sevoflurane and other volatile anaesthetics on heart rate in animals, human volunteers and patients (Ebert *et al.*, 1995a). Sevoflurane produces an increase in heart rate in chronically instrumented dogs but does not appreciably alter heart rate in instrumented swine (Manohar and Parks, 1984; Bernard *et al.*, 1990). On the other hand, in healthy volunteers, sevoflurane inhalation is associated with stable and unchanged heart rate (Holaday and Smith, 1981; Malan *et al.*, 1995; Ebert *et al.*, 1995b), whereas there are small but discernible changes in heart rate from awake baseline value during sevoflurane anaesthesia in children and adult patients during surgical operations (Frink *et al.*, 1992; Lerman *et al.*, 1994; Smith *et al.*, 1996). It is highly likely that these clinical data are influenced by many factors such as surgical procedures, neuronal reflexes, drug interactions, and changes in arterial blood P_{O2}, P_{CO2} and pH. Most of these factors seem to alter sympathetic and parasympathetic nerve activity and thereby secondarily affect the heart rate during sevoflurane inhalation.

To elucidate the direct effect of volatile anaesthetics on SA node function without these secondary influences, experiments on isolated SA node tissue or cells are required. Previous electrophysiological studies with microelectrode transmembrane recordings have clearly shown that halothane, enflurane and isoflurane moderately decelerate the spontaneous beating rate of guinea-pig SA node tissue (Bosnjak and Kampine, 1983). However, there is little information concerning the effect of these volatile anaesthetics on ionic currents contributing to SA node automaticity. Furthermore, the direct effect of the commonly used inhalational anaesthetic sevoflurane on SA node automaticity has yet to be fully elucidated.

The present electrophysiological study using isolated guinea-pig SA node cells provides the first detailed evidence that sevoflurane at clinically relevant concentrations produces moderate slowing of SA node automaticity, which may be at least partly due to its inhibitory action on I_f, $I_{Ca,T}$ and $I_{Ca,L}$.

Methods

SA node cell preparation

All animal care and experimental procedures complied with the Guide for the Care and Use of Laboratory Animals published by the US National Institutes of Health (NIH Publication No. 85-23, revised 1996) and were approved by the institution's Animal Care and Use Committee (2010-12-5). A total of 28 female Hartley guinea-pigs (5-8 weeks old, 250–400 g) were used in the work described here. All studies involving animals are reported in accordance with the ARRIVE guidelines for reporting experiments involving animals (McGrath et al., 2010).

Single SA node cells were isolated using an enzymatic dispersion procedure similar to that described previously (Guo *et al.*, 1997; Matsuura *et al.*, 2002). Briefly, guinea-pigs were deeply anaesthetized with sodium pentobarbital (i.p., 120 $mg \cdot kg^{-1}$), and then the chest cavity was opened under artificial respiration. The ascending aorta was cannulated *in situ* and the heart was then excised and retrogradely perfused via the aortic cannula on a Langendorff apparatus at 37°C, initially for 4 min with normal Tyrode solution containing (in mM) 140 NaCl, 5.4 KCl, 1.8 $CaCl_2$, 0.5 $MgCl_2$, 0.33 NaH_2PO_4, 5.5 glucose and 5 HEPES (pH adjusted to 7.4 with NaOH), and then for 4 min with nominally Ca^{2+}-free Tyrode solution (made by simply omitting $CaCl_2$ from the normal Tyrode solution). This was followed by 8–12 min of perfusion with nominally Ca^{2+}-free Tyrode solution containing 0.4 $mg \cdot mL^{-1}$ collagenase (Wako Pure Chemical Industries, Osaka, Japan). All these solutions were oxygenated with 100% O_2. The digested heart was then removed from the Langendorff apparatus, and the SA node region, bordered by the crista terminalis, the intra-atrial septum, and superior and inferior vena cava, was dissected out and cut perpendicular to the crista terminalis into small strips measuring about 0.5 mm in width. These SA node tissue strips were further digested at 37°C for 20 min with nominally Ca^{2+}-free Tyrode solution containing 1.0 $mg \cdot mL^{-1}$ collagenase (Wako) and 0.1 $mg \cdot mL^{-1}$ elastase (Wako). Finally, the enzymatically digested SA node strips were gently agitated in a high-K^+, low-Cl^- Kraftbrühe (KB) solution, containing (in mM) 70

K-glutamate, 30 KCl, 10 KH_2PO_4, 1 $MgCl_2$, 20 taurine, 0.3 EGTA, 10 glucose and 10 HEPES (pH adjusted to 7.2 with KOH) (Isenberg and Klöckner, 1982). The isolated cells thus obtained were then stored at 4°C in the KB solution for experimental use within 8 h.

Whole-cell patch-clamp recordings

Perforated and conventional (ruptured) whole-cell patch-clamp techniques were used to record the spontaneous action potentials and membrane currents (I_f, $I_{Ca,T}$, $I_{Ca,L}$ and I_{Ks}) in the current- and voltage-clamp modes respectively (Hamill *et al.*, 1981; Horn and Marty, 1988). An EPC-8 patch-clamp amplifier (HEKA, Lambrecht, Germany) was used for these recordings. The fire-polished patch electrodes had resistance of 2.0–4.0 MΩ when filled with the pipette solution. An aliquot of dissociated cells was transferred to a recording chamber (0.5 mL in volume) mounted on the stage of an inverted microscope (TMD300, Nikon, Tokyo) and was superfused at 35–37°C with normal Tyrode solution. Cells dissociated from the entire SA node region comprised morphologically heterogeneous cells, such as spindle- and spider-shaped cells. Because spindle-shaped cells closely resemble the primary pacemaker cells in the SA node (Belardinelli *et al.*, 1988), such cells displaying regular contraction were selected for the present experiments to assess the effect of sevoflurane on SA node electrical activity.

Spontaneous action potentials were recorded in normal Tyrode solution with a pipette solution containing (in mM) 70 potassium aspartate, 50 KCl, 10 KH_2PO_4, 1 $MgSO_4$ and 5 HEPES (pH adjusted to 7.2 with KOH). Amphotericin B (100 $\mu g \cdot mL^{-1}$, Wako) was added to the pipette solution just before use and measurements were started 5–10 min after giga-seal formation. In some experiments, spontaneous action potentials were recorded in the presence of zatebradine (Sigma, St Louis, MO, USA), $NiCl_2$ (Nacalai Tesque, Kyoto, Japan) or nifedipine (Sigma). Stock solutions were made either in distilled water (zatebradine, 1 mM; $NiCl_2$, 1 M) or in dimethyl sulfoxide (nifedipine, 20 mM), and were diluted in normal Tyrode solution for experimental use.

I_f was recorded in normal Tyrode solution with a K^+-rich pipette solution containing (in mM) 70 potassium aspartate, 50 KCl, 10 KH_2PO_4, 1 $MgSO_4$, 5 ATP (disodium salt; Sigma), 0.1 GTP (dilithium salt; Roche Diagnostics GmbH, Mannheim, Germany), 5 EGTA, 1.2 $CaCl_2$ and 5 HEPES (pH adjusted to 7.2 with KOH; pCa was estimated to be 7.3; Fabiato and Fabiato, 1979; Tsien and Rink, 1980). I_f was activated by hyperpolarizing voltage-clamp steps applied from a holding potential of –40 mV to test potentials of –50 to –140 mV and was measured as a time-dependent increase in inward current during the hyperpolarizing steps (Rigg *et al.*, 2003). During this hyperpolarization, I_f was typically recorded after an instantaneous current jump of small amplitude in inward direction, which indicates that the inward rectifier K^+ current was absent or very small in SA node cells (van Ginneken and Giles, 1991; Guo *et al.*, 1997; Matsuura *et al.*, 2002). The I_f conductance (g_f) was calculated at each test potential according to the following equation: $g_f = I_f/(V_t - V_{rev})$, where I_f is current density, V_t is test potential and V_{rev} is current reversal potential. The voltage dependence of I_f activation was assessed by fitting I_f conductance (g_f) to a Boltzmann equation: $g_f = 1/(1 + \exp((V_t - V_{1/2})/k))$, where $V_{1/2}$ is the voltage at half-maximal activation and k is the slope factor. When fully activated current-voltage (*I-V*) relationship for I_f was measured by its tail current, 2 mM $NiCl_2$ and 0.5 mM $BaCl_2$ were added to normal Tyrode solution to eliminate the voltage-dependent Ca^{2+} current and the Ba^{2+}-sensitive component of K^+ current respectively.

$I_{Ca,T}$ and $I_{Ca,L}$ were measured with a Cs^+-rich pipette solution containing (in mM) 90 cesium aspartate, 30 CsCl, 20 tetraethylammonium chloride, 2 $MgCl_2$, 5 ATP (Mg salt; Sigma), 5 phosphocreatine (disodium salt; Sigma), 0.1 GTP (dilithium salt; Roche), 5 EGTA and 5 HEPES (pH adjusted to 7.2 with CsOH; pCa was estimated to be 9.5; Fabiato and Fabiato, 1979; Tsien and Rink, 1980). The bath solution was a Na^+/K^+-free solution supplemented with tetrodotoxin (TTX, Wako), which contained (in mM) 140 Tris-hydrochloride, 1.8 $CaCl_2$, 0.5 $MgCl_2$, 5.5 glucose, 0.02 TTX and 5 HEPES (pH adjusted to 7.4 with Tris-base). An SA node cell was initially depolarized from a holding potential of –90 mV to various test potentials of –60 to +50 mV in 10 mV steps to activate the voltage-dependent Ca^{2+} current (I_{Ca}, composed of $I_{Ca,T}$ and $I_{Ca,L}$), and then was depolarized from a holding potential of –60 mV to test potentials of –50 to +50 mV in 10 mV steps to activate $I_{Ca,L}$. $I_{Ca,T}$ was determined as the difference current obtained by digital subtraction of $I_{Ca,L}$ from I_{Ca} at each test potential of –50 to +50 mV ($I_{Ca,T}$ at –60 mV was determined as membrane current activated using a holding potential of –90 mV without subtraction). The amplitude of $I_{Ca,T}$ and $I_{Ca,L}$ was measured as peak inward current level. The conductance for $I_{Ca,T}$ and $I_{Ca,L}$ was obtained by dividing the current amplitude at each test potential by the driving force and was normalized with the maximum value at +20 mV. The normalized conductance was fitted with a Boltzmann equation: $g_{Ca,L}$ (or $g_{Ca,T}$) $= 1/(1 + \exp((V_{1/2} - V_t)/k))$, where $V_{1/2}$ is the voltage at half-maximal activation, V_t is test potential and k is the slope factor.

I_{Ks} was measured with the K^+-rich pipette solution during superfusion with normal Tyrode solution supplemented with 5 μM E-4031 (Wako) and 0.4 μM nisoldipine (Sigma) to block I_{Kr} and $I_{Ca,L}$ respectively (Matsuura *et al.*, 2002). Stock solutions were made either in distilled water (E-4031, 5 mM) or in ethanol (nisoldipine, 1 mM) and were diluted in normal Tyrode solution. I_{Ks} was activated by depolarizing steps applied from a holding potential of –50 mV to test potentials of –40 to +40 mV and its activation was evaluated by measuring the amplitude of tail current elicited upon repolarization to the holding potential. Voltage dependence of I_{Ks} activation was evaluated by fitting the amplitude of tail current density ($I_{Ks,tail}$) with a Boltzmann equation: $I_{Ks,tail} = I_{Ks,tail,max}/(1 + \exp((V_{1/2} - V_t)/k))$, where $I_{Ks,tail,max}$ is the fitted maximal tail current density.

In experiments measuring the effects of sevoflurane on I_f, $I_{Ca,T}$, $I_{Ca,L}$ and I_{Ks}, sevoflurane was usually superfused during application of trains of activating steps for these currents, and the effect of sevoflurane was determined when a steady-state response was obtained.

All potentials were off-line corrected for a liquid junction potential of 10 mV between the aspartate-rich pipette solutions (K^+- and Cs^+-rich pipette solution) and bath solutions. The voltage-clamp protocols and data acquisition were controlled with PATCHMASTER software (HEKA), and current records were low-pass filtered at 1 kHz, digitized at 2 kHz through an LIH-1600 interface (HEKA) and stored on a computer. Cell membrane capacitance (C_m) was calculated for each cell from the capacitive transient elicited by 20 ms voltage-clamp steps (±5 mV) according to the following equation: $C_m = \tau_C I_0/\Delta V_m(1 - I_\infty/I_0)$, where τ_C is the time constant of the capacitive transient, I_0 is the initial peak current amplitude, I_∞ is the steady-state current value and ΔV_m is the amplitude of voltage step (Bénitah *et al.*, 1993). The sampling rate for these measurements of C_m was 50 kHz with a low-pass 10 kHz filter. The average values for C_m in SA node cells used in the present study were 41.1 ± 1.2 pF (mean ± SEM; $n = 64$ cells). To account for differences in cell size, the current amplitude was presented as current density (in pA·pF^{-1}), obtained by normalizing with reference to C_m. The zero-current level is indicated to the left of the current records by a horizontal line, while the zero-potential level is denoted by a dashed line.

Administration of sevoflurane

Sevoflurane (Abbott Laboratories, North Chicago, IL, USA) was equilibrated in extracellular solutions in a reservoir by passing air (flow rate, 0.5 L·min^{-1}) through a calibrated vaporizer for at least 15 min before experiments. The mM concentrations of sevoflurane in bath solutions were measured to be 0.12, 0.32, 0.44, 0.58 and 0.71 mM by gas chromatography, when delivered via vaporizer at volume percentages of 1, 2, 3, 4 and 5% of sevoflurane respectively (Kojima *et al.*, 2011). These ranges in mM concentrations of sevoflurane are equivalent to the blood concentrations reported in patients during sevoflurane anaesthesia (Frink *et al.*, 1992; Matsuse *et al.*, 2011; refer to Discussion). In the present experiments, sevoflurane concentration is expressed as mM concentrations throughout, except for the experiments of sevoflurane inhalation *in vivo* where sevoflurane concentration is expressed as volume percentage.

Measurement of heart rate in Langendorff mode

Hearts were rapidly excised from guinea-pigs, mounted on a Langendorff perfusion apparatus and perfused at a constant pressure of 60 mmHg at 37°C with normal Tyrode solution oxygenated with 100% O_2. ECG was recorded via two silver electrodes attached to the ventricular apex and to the aortic cannula. An equilibration period of approximately 30 min was allowed to ensure the stable ECG recordings. The hearts were then successively perfused with sevoflurane at concentrations of 0.12, 0.44 and 0.71 mM for 10 min with intervening washout periods of 10 min. It should be noted that the effect of sevoflurane on heart rate was almost completely reversed during the washout period.

Measurement of heart rate in vivo

Guinea-pigs were initially anaesthetized with sodium pentobarbital (i.p., 80 mg·kg^{-1}) and were artificially ventilated through a tracheotomy with a respirator [tidal volume, 2.5 mL; rate, 60 min^{-1}; flow rate, 0.5 L·min^{-1} of an air-oxygen mixture (60% inspired oxygen)]. Surface ECG was recorded by placing wire electrodes in subcutaneous spaces in a lead II configuration. A period of approximately 30 min was allowed for the stabilization of surface ECG recordings, and sevoflurane was then successively administered in 0.5 L·min^{-1} of an air-oxygen mixture, at concentrations of 1, 3 and 5% in a randomized order for a period of 10–20 min for each concentration. ECG data were recorded from Langendorff and *in vivo* hearts using PowerLab data acquisition system and LabChart 7 software (ADInstruments, Castle Hill, Australia).

Computer simulation of spontaneous action potentials

The Kurata SA node model (Kurata *et al.*, 2002) was coded by simBio (Sarai *et al.*, 2006) and was used for the computer simulation study. The spontaneous action potentials of SA node cells in the presence of sevoflurane were simulated by decreasing the conductances for I_f, $I_{Ca,T}$, $I_{Ca,L}$ and/or I_{Ks}, which were measured by the present voltage-clamp experiments, without altering other parameters. Changes in firing rate, diastolic depolarization rate (DDR), maximum diastolic potential (MDP), action potential amplitude (APA) and maximum upstroke velocity (max dV·dt^{-1}) were compared between the experimental and simulated action potential data.

Statistical analysis

Results are expressed as the means ± SEM, with the number of animals (cell isolations) and cells from which measurements were made indicated by *N* and *n* respectively. Statistical comparisons were analysed using either one-way ANOVA followed by Dunnett's test or repeated measure ANOVA followed by Newman–Keuls test (GraphPad Prism 5, La Jolla, CA, USA). All statistical tests were two tailed. A value of $P < 0.05$ was regarded as statistically significant.

Results

Inhibitory effect of sevoflurane on spontaneous activity in SA node cells

Figure 1 shows the results of a representative experiment examining the effect of clinically relevant concentrations of sevoflurane on spontaneous action potentials, with the use of the amphotericin B-perforated patch-clamp technique. An SA node cell was successively exposed to sevoflurane at concentrations of 0.12, 0.32, 0.44, 0.58 and 0.71 mM for 5–8 min, with a washout interval of about 5–6 min between each exposure (Figure 1A). As demonstrated in the lower panel of Figure 1A, firing rate of spontaneous action potentials was reduced during exposure to sevoflurane at each concentration, which then almost completely recovered to the initial baseline level after washout of sevoflurane. Figure 1B–H illustrates action potentials (upper panels) and their first derivatives (dV·dt^{-1}, lower panels) on an expanded timescale recorded before (control) and during exposure to sevoflurane at each concentration, and after washout of 0.71 mM sevoflurane. Action potentials are characterized by the presence of diastolic depolarization that leads to smooth transition into the upstroke of the next action potential. Under control conditions, the parameters for spontaneous action potentials are shown in Table 1 and Figure 2. These parameters except action potential duration measured from the peak to 50% and 90% repolarization (APD_{50} and APD_{90}, respectively) were significantly altered by the higher concentrations (0.44 mM or greater) of sevoflurane.

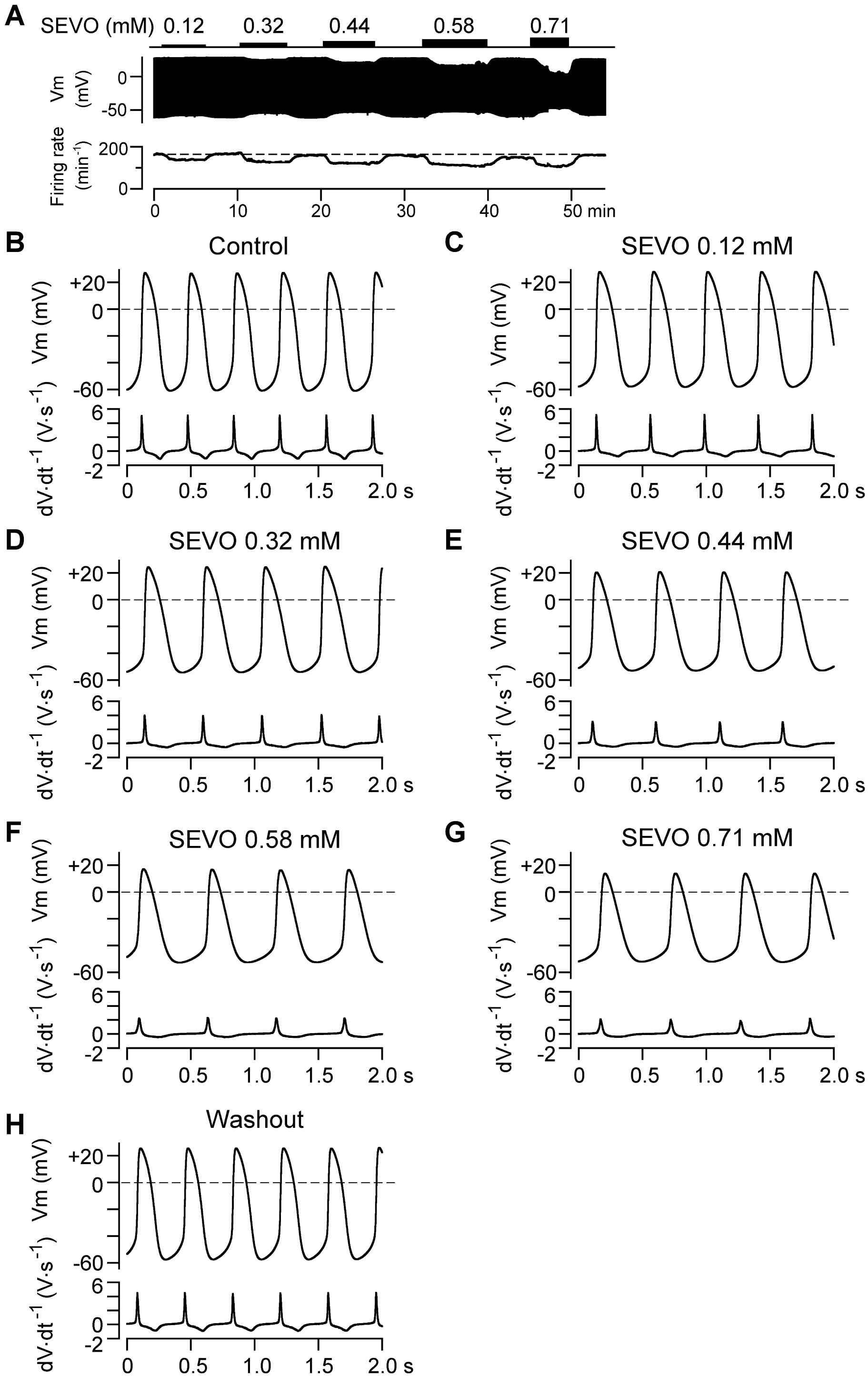

Figure 1

Effect of sevoflurane (SEVO) on spontaneous action potentials in guinea-pig SA node cell. (A) Continuous recording of spontaneous action potentials during 5–8 min administration of sevoflurane at concentrations of 0.12, 0.32, 0.44, 0.58 and 0.71 mM with 5–6 min of washout period (upper panel). Simultaneous measurement of spontaneous firing rate plotted on the same timescale as in the action potential recordings, with a dashed line indicating an initial baseline value of 163 min^{-1} (lower panel). Sevoflurane was administered until the response of action potential amplitude and spontaneous firing rate reached steady-state levels. The periods of administration of sevoflurane are noted above the recording of action potentials. (B–H) Action potentials (upper panel) and their first derivatives ($dV \cdot dt^{-1}$, lower panel) on an expanded timescale, recorded under control conditions (B) and during exposure to sevoflurane at concentrations of 0.12 mM (C), 0.32 mM (D), 0.44 mM (E), 0.58 mM (F), and 0.71 mM (G), and after washout of 0.71 mM sevoflurane (H).

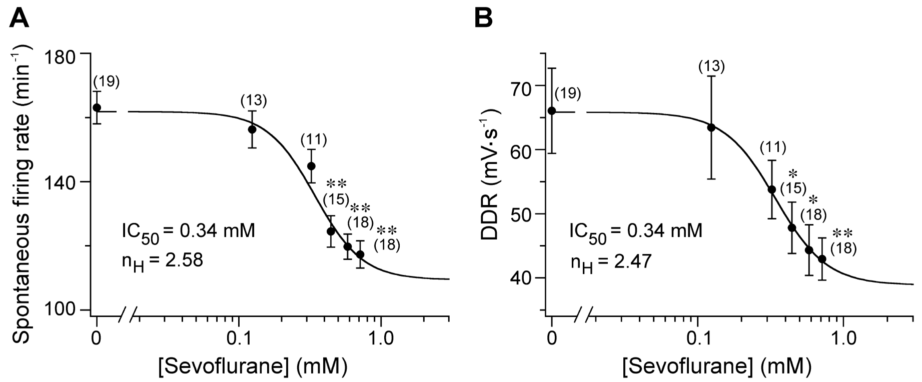

Figure 2

Similar concentration dependence for the effects of sevoflurane on spontaneous firing rate and DDR. Spontaneous firing rate (A) and DDR (B) plotted against concentrations of sevoflurane (mM). DDR was measured as the slope of diastolic depolarization over the first two-thirds of the diastolic interval where it showed approximately constant value. The data points were fitted by a Hill equation: $R = R_0/(1 + ([\text{Sevoflurane}]/IC_{50})^{nH})$, where R is the spontaneous firing rate (panel A) or DDR (panel B), R_0 is the estimated value for the spontaneous firing rate (panel A) or DDR (panel B) without sevoflurane, IC_{50} is the concentration of sevoflurane causing a half-maximal response and n_H is a Hill coefficient. The data were reasonably well described by a Hill equation, yielding IC_{50} of 0.34 mM and n_H of 2.58 for spontaneous firing rate (A), and IC_{50} of 0.34 mM and n_H of 2.47 for DDR (B). Sevoflurane was tested at two to five concentrations per cell in the range of 0.12–0.71 mM with a washout period of 5–6 min between each application. Data were included in the analysis when sevoflurane effect was almost completely recovered to the initial baseline level, which was used as control. The number of cells is shown in parenthesis, obtained from 5 different cell isolations ($N = 5$). $^*P < 0.05$ and $^{**}P < 0.01$ compared with control.

Figure 3

Slowing of spontaneous activity of guinea-pig SA node cells by zatebradine. (A) Superimposed action potentials recorded before and during exposure to increasing concentrations of zatebradine (0.1 and 1 μM) in a cumulative manner, with each concentration applied for 10–15 min. (B,C) Summarized data for spontaneous firing rate (B) and DDR (C) before and during exposure to 0.1 and 1 μM zatebradine. The number of cells is shown in parenthesis, obtained from 3 different cell isolations ($N = 3$). $^*P < 0.05$ and $^{**}P < 0.01$ compared with control.

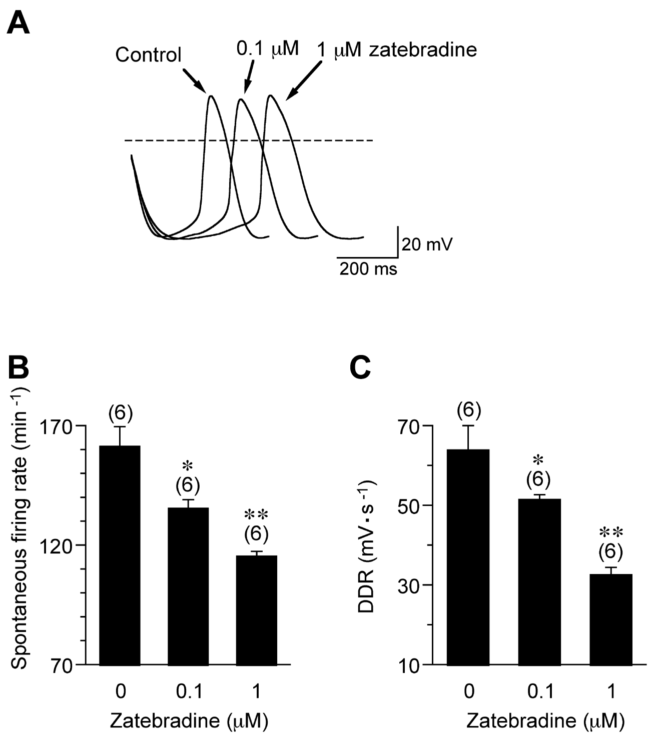

We then focused on analysing the concentration-dependent effect of sevoflurane on spontaneous firing rate and its important electrophysiological determinant DDR (Honjo *et al.*, 1996; Verkerk *et al.*, 2009). As illustrated in Figure 2A, sevoflurane decreased the spontaneous firing rate in a concentration-dependent manner with a half-maximal IC_{50} of 0.34 mM and Hill coefficient (n_H) of 2.58. Notably, DDR was also reduced by sevoflurane with a qualitatively similar concentration dependence with an IC_{50} of 0.34 mM and n_H of 2.47 (Figure 2B). These similarities indicate that sevoflurane slowed the spontaneous firing rate primarily by decreasing DDR. Sevoflurane was thus found to directly decelerate SA node automaticity when applied over a range of clinically used concentrations.

Inhibitory effect of sevoflurane on I_f in SA node cells

To elucidate the ionic basis for the negative chronotropic effect of sevoflurane, we examined the effect of sevoflurane on four major ionic currents (I_f, $I_{Ca,T}$, $I_{Ca,L}$ and I_{Ks}) that contribute to the electrical activity of SA node cells. During the course of these voltage-clamp experiments, we used a sevoflurane concentration of 0.44 mM as a standard test concentration, because this concentration is high enough to significantly reduce both spontaneous firing rate and DDR (Figure 2).

It has been demonstrated that I_f activity constitutes one of the main factors controlling DDR and spontaneous firing rate in SA node pacemaker cells of various mammalian species

Table 1

Parameters of spontaneous action potentials in the absence and presence of sevoflurane

	Control (*n* = 19)	Sevoflurane 0.12 mM (*n* = 13)	0.32 mM (*n* = 11)	0.44 mM (*n* = 15)	0.58 mM (*n* = 18)	0.71 mM (*n* = 18)
APA (mV)	85.5 ± 1.3	83.0 ± 1.6	75.6 ± 2.9	71.1 ± 3.3**	68.0 ± 3.6**	60.9 ± 2.8**
APD_{50} (ms)	96.1 ± 2.3	101.5 ± 6.1	96.1 ± 7.9	93.2 ± 8.4	93.1 ± 7.8	89.1 ± 6.5
APD_{90} (ms)	150.3 ± 2.6	161.1 ± 6.6	160.5 ± 8.1	162.9 ± 10.3	157.7 ± 10.5	163.3 ± 8.5
MDP (mV)	–60.4 ± 0.9	–58.8 ± 0.9	–57.1 ± 1.9	–55.2 ± 1.7	–55.6 ± 1.8	–53.2 ± 1.9**
max $dV{\cdot}dt^{-1}$ ($V{\cdot}s^{-1}$)	9.3 ± 2.0	7.5 ± 1.6	5.2 ± 1.4	4.4 ± 1.1*	3.8 ± 0.7**	2.5 ± 0.5**

Data are presented as mean ± SEM, and the number of experiments is shown in parenthesis (data are from same experiments as shown in Figure 2, $N = 5$). $^{*}P < 0.05$, $^{**}P < 0.01$ compared with control.

APA, action potential amplitude; APD_{50}, action potential duration measured from the peak to 50% repolarization; APD_{90}, action potential duration measured from the peak to 90% repolarization; MDP, maximal diastolic potential; max $dV{\cdot}dt^{-1}$, maximum rate of rise of the action potential.

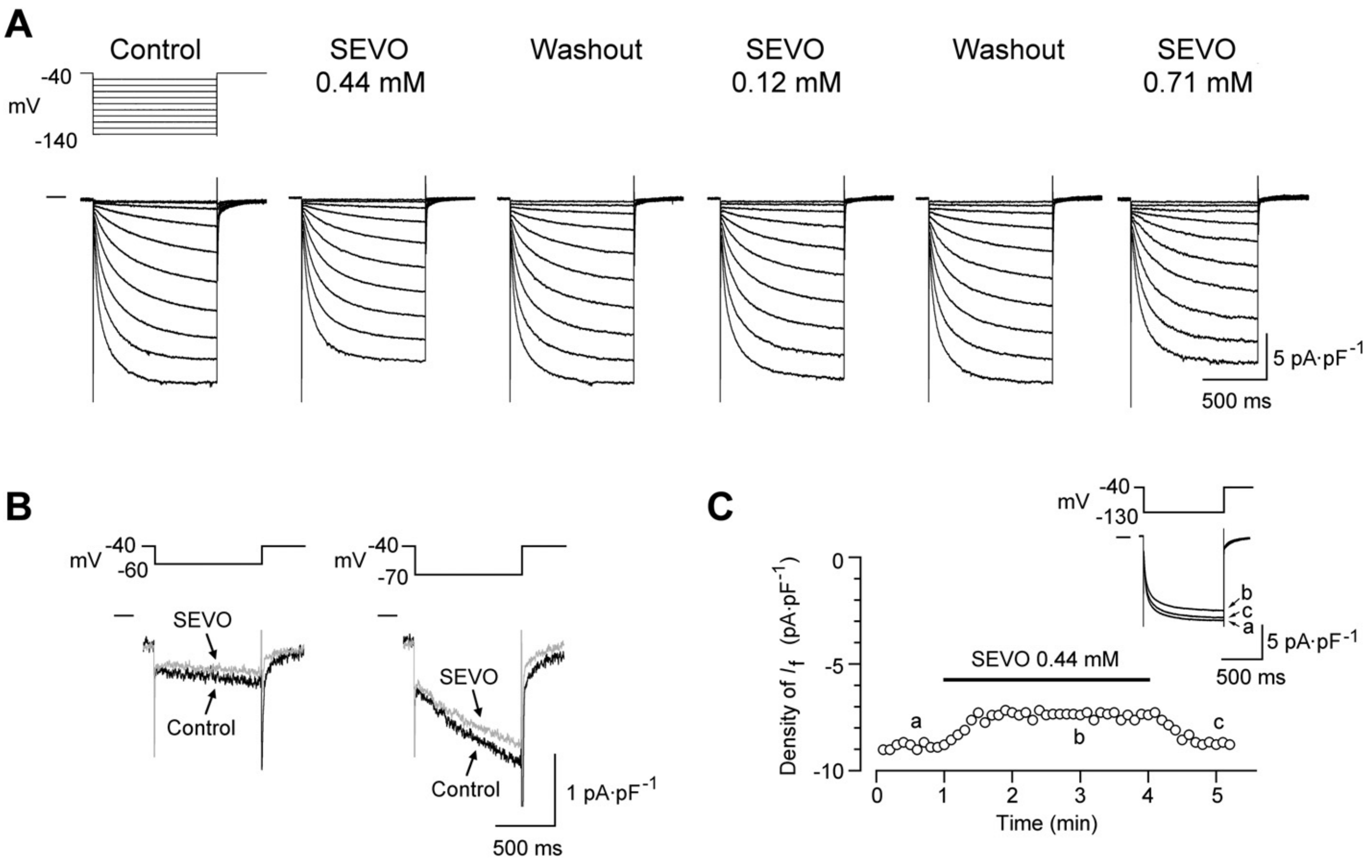

Figure 4

Reduction of I_f by sevoflurane (SEVO). (A) Superimposed current traces of I_f, activated during 1 s hyperpolarizing steps to potentials of –50 to –140 mV applied from a holding potential of –40 mV during sequential administration of 0.44, 0.12 and 0.71 mM of sevoflurane for 3–5 min with a washout period of approximately 5 min between each application. (B) I_f at test potentials of –60 and –70 mV before (control) and during (SEVO) exposure to 0.44 mM sevoflurane, shown on an expanded current scale. These traces are from panel A. (C) Time course of changes in the amplitude of I_f during exposure to 0.44 mM sevoflurane. I_f was repetitively (every 6 s) activated by hyperpolarizing voltage steps to –130 mV applied from a holding potential of –40 mV.

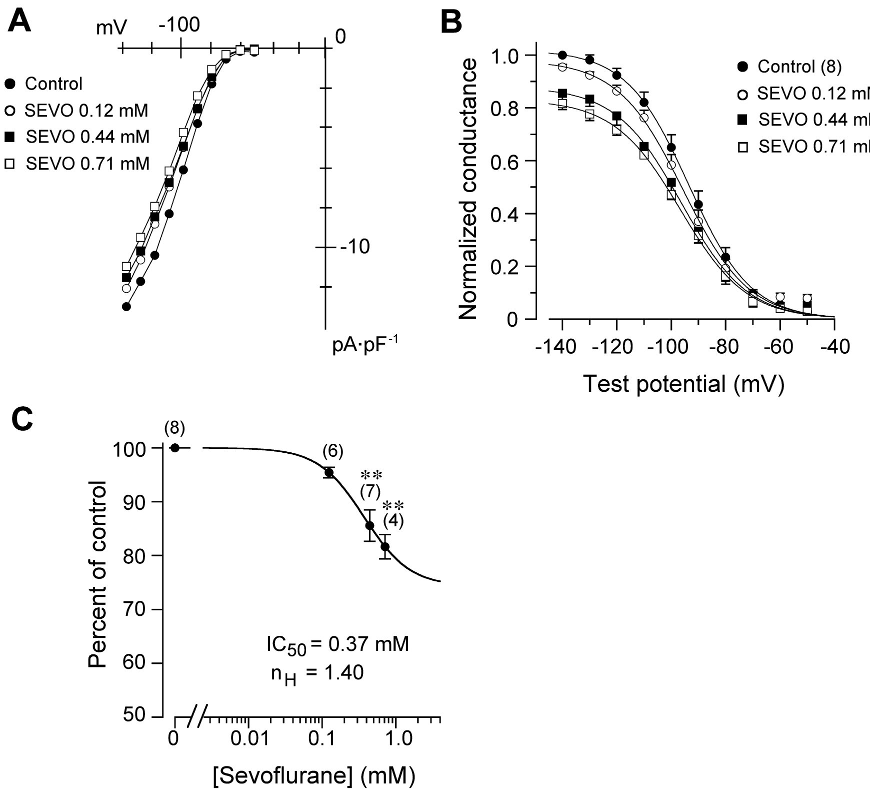

Figure 5

Inhibitory effect of sevoflurane (SEVO) on I_f at the quasi-steady-state activation. (A) Quasi-steady-state *I-V* relationships for I_f in control and during administration of 0.12, 0.44 and 0.71 mM of sevoflurane, obtained from current traces shown in Figure 4A. I_f was measured as the difference between initial and late current levels recorded at the onset and end of voltage steps respectively. (B) Normalized I_f conductance–voltage relationships measured at the quasi-steady-state in the absence and presence of 0.12, 0.44 and 0.71 mM sevoflurane. Conductance at each test potential in control and in the presence of sevoflurane was normalized with reference to the maximum conductance obtained at –140 mV in control. The smooth curves through the data points represent a least-squares fit with a Boltzmann equation, yielding $V_{1/2}$ and k (see Table 2). (C) Concentration-dependent reduction of I_f conductance by sevoflurane. I_f conductance at –140 mV in the presence of 0.12, 0.44 and 0.71 mM of sevoflurane was normalized with the control value at –140 mV and was fitted with a Hill equation, yielding an IC_{50} of 0.37 mM and n_H of 1.40. **$P < 0.01$ compared with control. In the experiments shown in panels B and C, the effect of sevoflurane on I_f was tested at several concentrations only when the inhibitory effect of the previous concentration was readily and almost completely reversed after the washout. The number of experiments is shown in parenthesis (N = 3).

(DiFrancesco, 1991; DiFrancesco, 1993; Dobrzynski *et al.*, 2007; Mangoni and Nargeot, 2008; Verkerk *et al.*, 2009; Baruscotti *et al.*, 2010). Zatebradine blocks I_f in SA node cells in a concentration-dependent manner (IC_{50} of 0.48 μM) and with minimal effect on other ionic currents such as $I_{Ca,L}$ and delayed rectifier K^+ current at a concentration of 1 μM (Goethals *et al.*, 1993; Baruscotti *et al.*, 2005). We therefore evaluated the functional role of I_f in electrical activity of guinea-pig SA node cells by examining the effect of zatebradine at concentrations of 0.1 and 1 μM. Spontaneously active SA node cells were exposed to increasing concentrations of zatebradine (0.1 and 1 μM) in a cumulative manner. As demonstrated in Figure 3, zatebradine at both concentrations decreased the spontaneous firing rate, associated with a significant reduction of DDR. These results indicate that I_f contributes at least partly to the slope of diastolic depolarization and thereby firing frequency of spontaneous action potentials in guinea-pig SA node cells, consistent with previous studies on the same species (BoSmith *et al.*, 1993; Thollon *et al.*, 2007).

We then investigated the effect of sevoflurane on conductance, selectivity and kinetic properties of I_f (Figures 4–7). Figure 4A illustrates superimposed current traces in response to hyperpolarizing steps to test potentials of –50 to –140 mV, recorded during the successive administration of three different concentrations (0.44, 0.12 and 0.71 mM) of sevoflurane for 3–5 min with a washout period of approximately 5 min. I_f was appreciably activated at test potentials of –60 and –70 mV (Figure 4B), where the diastolic depolarization develops, and was moderately inhibited by 0.44 mM sevoflurane. As illustrated in Figure 4C, we confirmed in different sets of experiments that sevoflurane at 0.44 mM rapidly and reversibly inhibited I_f, repetitively activated by hyperpolarizing steps to –130 mV. It should be noted that because I_f activation did not reach the steady-state levels within 1 s of voltage steps to less hyperpolarized potentials of –60 to –110 mV, the present experiments evaluated the effects of sevoflurane on I_f at the quasi-steady-state activation in these potential ranges.

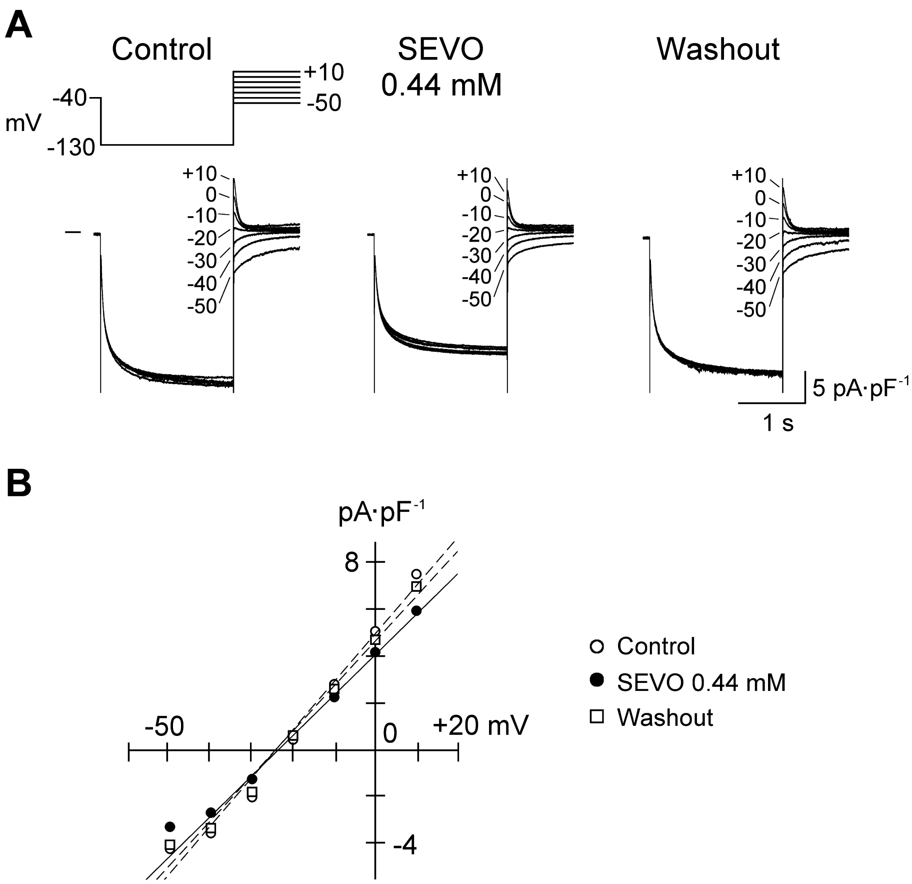

Figure 6

Fully activated *I-V* relationships for I_f. (A) The membrane potential was hyperpolarized to –130 mV for 2 s and was then stepped back to various test potentials of +10 to –50 mV in 10 mV steps, before and 5 min after exposure to 0.44 mM sevoflurane (SEVO), and after 5 min of washout, obtained in the same cell. (B) *I-V* relationships for tail currents recorded at test potentials before (open circles) and during (filled circles) exposure to 0.44 mM sevoflurane, and after washout (open squares). The straight lines represent linear regression fits to the data points.

Table 2

Parameters of voltage-dependent activation for I_f, $I_{Ca,T}$, $I_{Ca,L}$ and I_{Ks} in the absence and presence of sevoflurane

			Sevoflurane		
		Control	**0.12 mM**	**0.44 mM**	**0.71 mM**
I_f	$V_{1/2}$ (mV)	–93.8 ± 2.4	–95.5 ± 2.1	–96.0 ± 1.9	–96.2 ± 1.6
	k (mV)	10.8 ± 0.4	11.4 ± 0.5	11.5 ± 0.4	11.8 ± 0.8
		(n = 8, N = 3)	(n = 6, N = 3)	(n = 7, N = 3)	(n = 4, N = 3)
$I_{Ca,T}$	$V_{1/2}$ (mV)	–42.8 ± 1.2		–43.9 ± 2.7	–42.6 ± 2.8
	k (mV)	5.3 ± 0.7		5.1 ± 1.5	5.1 ± 0.5
		(n = 8, N = 3)		(n = 4, N = 2)	(n = 4, N = 2)
$I_{Ca,L}$	$V_{1/2}$ (mV)	–16.7 ± 1.4		–19.4 ± 1.7	–18.5 ± 3.2
	k (mV)	6.9 ± 0.6		5.8 ± 0.3	6.7 ± 0.6
		(n = 8, N = 3)		(n = 4, N = 2)	(n = 4, N = 2)
I_{Ks}	$V_{1/2}$ (mV)	17.7 ± 1.1		18.0 ± 1.1	18.8 ± 1.1
	k (mV)	14.0 ± 0.6		14.2 ± 0.7	13.1 ± 1.0
		(n = 6, N = 3)		(n = 6, N = 3)	(n = 4, N = 2)

Data are presented as mean ± SEM, and the number of experiments is shown in parenthesis. There are no significant differences in each parameter in the absence and presence of sevoflurane.
$V_{1/2}$, voltage at half-maximal activation; k, slope factor.

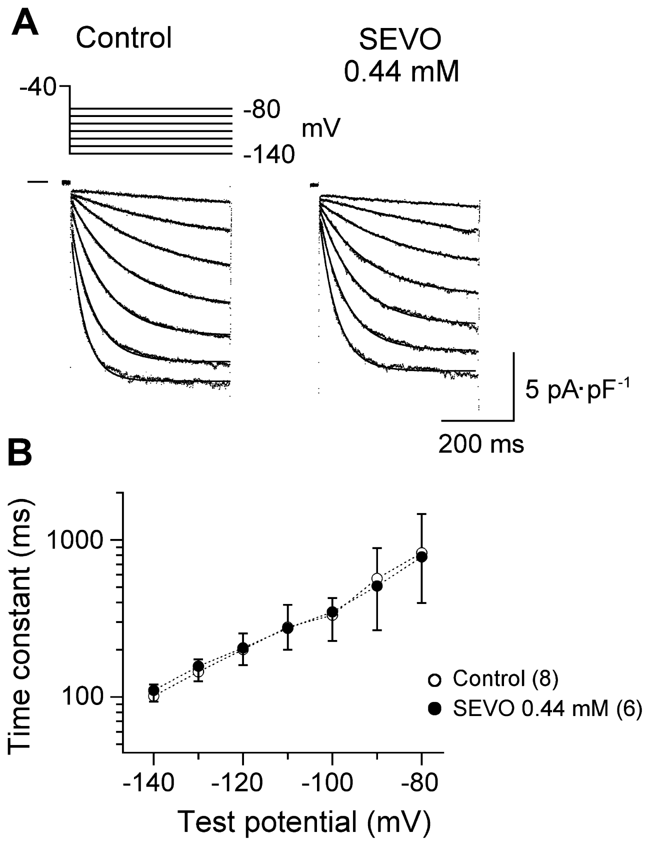

Figure 7

Effect of sevoflurane (SEVO) on the time course of I_f activation. (A) Single exponential fits (continuous curve) of I_f (dotted points), activated by hyperpolarizing steps to potentials of −80 to −140 mV before and 5 min after exposure to 0.44 mM sevoflurane. (B) Summarized data for the time constant of I_f activation in the absence and presence of sevoflurane. There are no significant differences between the control and sevoflurane groups at any test potentials. The number of cells is shown in parenthesis (N = 3 for both groups).

Figure 5A illustrates quasi-steady-state *I-V* relationships for I_f in the absence and presence of sevoflurane at concentrations of 0.12, 0.44 and 0.71 mM, shown in Figure 4A. I_f conductances in the absence and presence of sevoflurane were estimated at each test potential using the reversal potential of −24 mV, which was similar in both conditions (control, −24.1 ± 0.7 mV; 0.44 mM sevoflurane, −24.3 ± 0.8 mV, $n = 4$, $N = 2$; refer to Figure 6). Voltage dependence of I_f activation was evaluated by fitting the normalized I_f conductance with Boltzmann equation and was found to be little affected by sevoflurane at any concentrations tested (Table 2). Sevoflurane at concentrations of 0.12, 0.44 and 0.71 mM reduced the maximal I_f conductance determined at −140 mV by 4.6, 14.4 and 18.4% on average respectively (Figure 5B). Figure 5C illustrates the concentration-dependent reduction of I_f conductance by sevoflurane, which was reasonably well fitted by a Hill equation, yielding an IC_{50} of 0.37 mM and n_H of 1.40.

The fully activated *I-V* relationships for I_f were constructed by measuring the tail current amplitudes at various test potentials following 2 s hyperpolarizing steps to −130 mV before, during exposure to 0.44 mM sevoflurane and after its washout (Figure 6A). Figure 6B illustrates tail current densities plotted against the test potentials, with best-fit lines by linear regressions. The slope of *I-V* relationship reflects the fully activated I_f conductance at −130 mV, and in a total of four SA node cells, this slope was decreased by 15.8 ± 2.3% from 143.2 ± 15.8 to 119.9 ± 11.2 $pS{\cdot}pF^{-1}$ by 0.44 mM sevoflurane, confirming again an inhibitory action of sevoflurane on I_f. It should be noted that a similar reduction of I_f conductance was estimated when analysed by measuring the amplitude of I_f at a test potential of −130 mV in the absence and presence of 0.44 mM sevoflurane (15.1 ± 2.7% reduction, $n = 7$, $N = 3$; Figure 5B). The inhibitory effect of sevoflurane was also largely reversible after its washout (Figure 6). In addition, the reversal potential for I_f was not altered by sevoflurane, which suggests that ion selectivity for I_f was not affected by sevoflurane.

The activation time course of I_f at potentials of −80 to −140 mV, determined by fitting with single exponential function, was not also influenced by 0.44 mM sevoflurane (Figure 7).

Inhibitory effects of sevoflurane on $I_{Ca,T}$ and $I_{Ca,L}$ in SA node cells

There is good evidence that $I_{Ca,T}$ and $I_{Ca,L}$ play an important role in the electrical activities associated with SA node automaticity (Hagiwara *et al.*, 1988; Kodama *et al.*, 1997; Verheijck *et al.*, 1999; Mangoni *et al.*, 2003; 2006; Dobrzynski *et al.*, 2007; Mangoni and Nargeot, 2008). In the present experiments, the effects of sevoflurane on $I_{Ca,T}$ and $I_{Ca,L}$ were examined by using two different holding potentials of −90 and −60 mV (Hagiwara *et al.*, 1988; Mangoni and Nargeot, 2001). Because $I_{Ca,L}$ in SA node cells is largely conducted by $Ca_V1.3$ channel (Tellez *et al.*, 2006), which is activated at more hyperpolarized potentials compared with that of $Ca_V1.2$ channel-based $I_{Ca,L}$ (Lipscombe, 2002), depolarizing test steps to record $I_{Ca,L}$ were applied from a holding potential of −60 mV (Mangoni and Nargeot, 2001). Figure 8A illustrates original current traces of I_{Ca} (composed of $I_{Ca,T}$ and $I_{Ca,L}$) and $I_{Ca,L}$ recorded in the same SA node cell under control conditions and 5 min after administration of 0.44 mM sevoflurane. I_{Ca} and $I_{Ca,L}$ were activated by 200 ms depolarizing steps applied from holding potentials of −90 and −60 mV respectively. $I_{Ca,T}$ was obtained by digitally subtracting $I_{Ca,L}$ from I_{Ca} at each test potential (Figure 8B). Sevoflurane was found to inhibit both $I_{Ca,T}$ and $I_{Ca,L}$ (refer to Figure 9). We also examined the time courses for the action of 0.44 mM sevoflurane on $I_{Ca,T}$ and $I_{Ca,L}$ in different sets of experiments. Because the activation of $I_{Ca,L}$ was minimal at a test potential of −50 mV (Figure 8A), $I_{Ca,T}$ was measured at depolarizing steps to −50 mV applied from a holding potential of −90 mV. Sevoflurane caused rapid and reversible inhibition of $I_{Ca,T}$ (Figure 8C) and $I_{Ca,L}$ (activated by depolarizing steps to −10 mV applied from a holding potential of −60 mV; Figure 8D).

Figure 9A and B, respectively, demonstrate the inhibitory effects of sevoflurane on $I_{Ca,T}$ and $I_{Ca,L}$ at all test potentials. Under control conditions, amplitude of $I_{Ca,T}$ peaked at −30 mV (−3.5 ± 0.3 $pA{\cdot}pF^{-1}$, $n = 8$, $N = 3$), whereas $I_{Ca,L}$ exhibited a peak amplitude of −4.1 ± 0.4 $pA{\cdot}pF^{-1}$ ($n = 8$, $N = 3$) at −10 mV. These peak potentials of $I_{Ca,T}$ and $I_{Ca,L}$ are, respec-

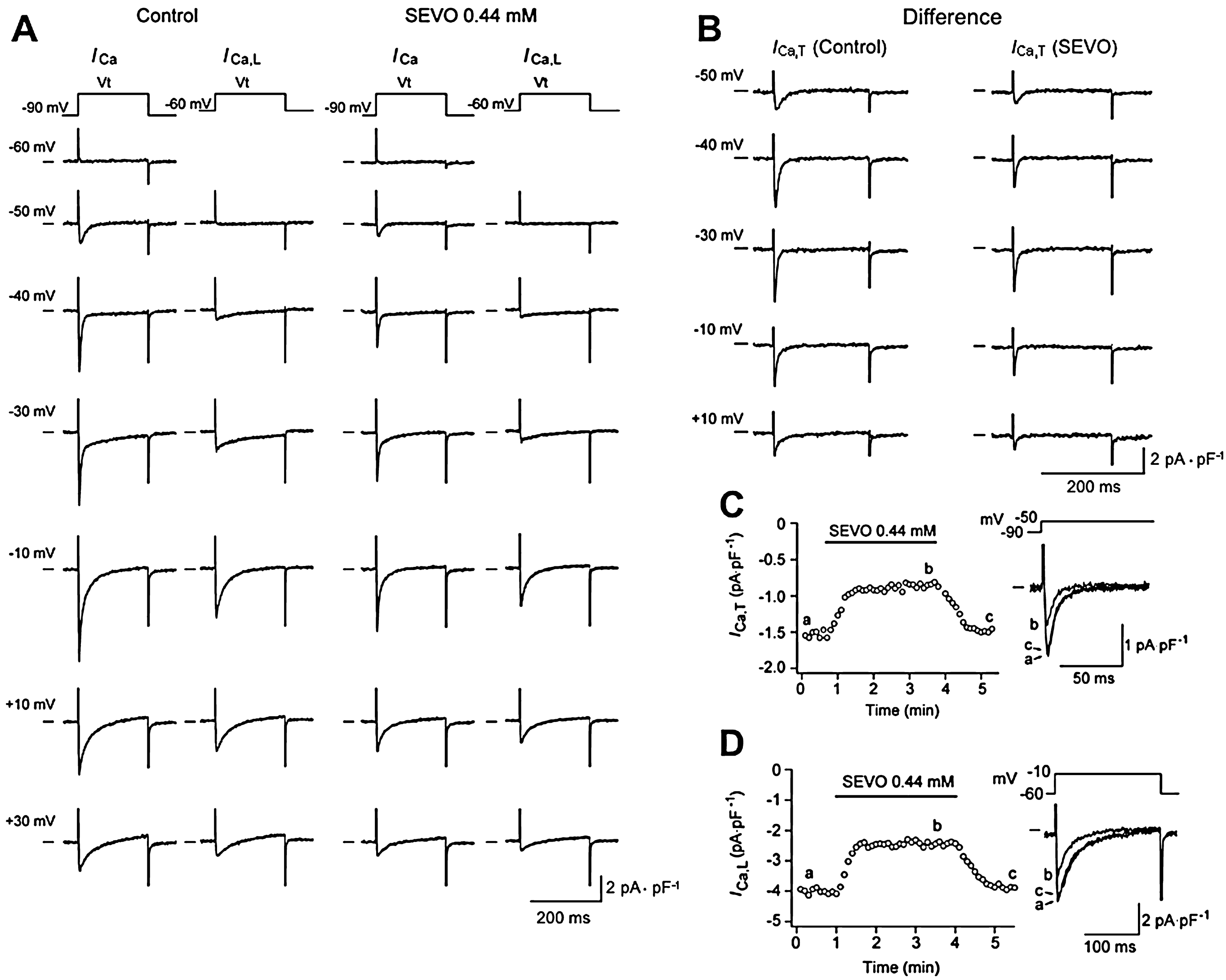

Figure 8

Reduction of $I_{Ca,T}$ and $I_{Ca,L}$ by sevoflurane (SEVO). (A) I_{Ca} and $I_{Ca,L}$ recorded under control conditions and during administration of sevoflurane. Depolarizing steps of 200-ms duration were applied initially from a holding potential of −90 mV to activate I_{Ca} and then from a holding potential of −60 mV to evoke $I_{Ca,L}$. These voltage-clamp protocols were repeated in the same SA node cells, before and 5 min after administration of 0.44 mM sevoflurane. (B) $I_{Ca,T}$ before and after administration of 0.44 mM sevoflurane, obtained by digitally subtracting $I_{Ca,L}$ from I_{Ca} at each test potential, shown in panel A. (C,D) Time courses of changes in amplitudes of $I_{Ca,T}$ (C) and $I_{Ca,L}$ (D) during administration of sevoflurane (0.44 mM) and after its washout, measured in different SA node cells. Inset shows voltage-clamp protocols (applied every 6 s) and superimposed current traces for $I_{Ca,T}$ (C) and $I_{Ca,L}$ (D) recorded at time points indicated by characters (a, b and c). Note that $I_{Ca,T}$ was measured during depolarizing steps to −50 mV applied from a holding potential of −90 mV, where the contamination of $I_{Ca,L}$ was minimal (refer to panel A).

tively, similar to those of $I_{Ca,T}$ and $I_{Ca,L}$ in mouse SA node cells (Mangoni and Nargeot, 2001). Sevoflurane at 0.44 and 0.71 mM significantly reduced the amplitudes of $I_{Ca,T}$ and $I_{Ca,L}$ at most test potentials. The inhibitory actions of sevoflurane on $I_{Ca,T}$ and $I_{Ca,L}$ were analysed by constructing the normalized conductance–voltage relationships fitted with Boltzmann equation. Sevoflurane at 0.44 and 0.71 mM reduced the maximal conductance of $I_{Ca,T}$ by 31.3 and 48.2% on average respectively (Figure 9C). On the other hand, sevoflurane at 0.44 and 0.71 mM decreased the maximal conductance of $I_{Ca,L}$ by 30.3 and 50.3% on average respectively (Figure 9D). The voltage dependences for activation of $I_{Ca,T}$ and $I_{Ca,L}$ were not significantly affected by sevoflurane (Table 2).

Functional roles of $I_{Ca,T}$ and $I_{Ca,L}$ in SA node pacemaking activity

We examined the roles of $I_{Ca,T}$ and $I_{Ca,L}$ in SA node pacemaking activity by using their respective inhibitors $NiCl_2$ and nifedipine. Figure 10A shows the superimposed spontaneous action potentials recorded before and 5 min after exposure to 40 μM $NiCl_2$, which has been shown to selectively block $I_{Ca,T}$ without appreciably affecting $I_{Ca,L}$ in SA node cells (Hagiwara *et al.*, 1988). As summarized in Figure 10B, 40 μM $NiCl_2$ mod-

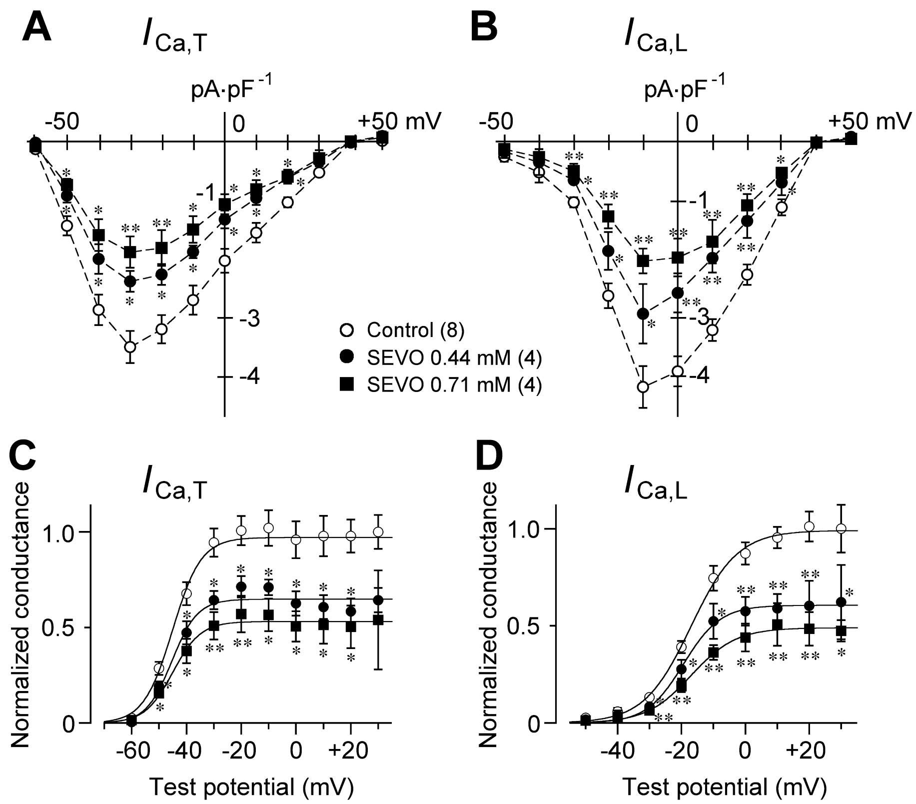

Figure 9

Inhibitory effects of sevoflurane (SEVO) on $I_{Ca,T}$ and $I_{Ca,L}$. (A,B) Mean *I-V* relationships for $I_{Ca,T}$ (A) and $I_{Ca,L}$ (B) in the absence (control) and presence of 0.44 and 0.71 mM sevoflurane. The number of cells is shown in parenthesis. (C,D) Normalized conductance–voltage relationships for $I_{Ca,T}$ (C) and $I_{Ca,L}$ (D) in the absence (control) and presence of 0.44 and 0.71 mM sevoflurane. Conductances for $I_{Ca,T}$ and $I_{Ca,L}$ at each test potential in control and in the presence of sevoflurane were normalized with reference to the maximum conductance obtained at +20 mV in control. The driving force for $I_{Ca,T}$ and $I_{Ca,L}$ was calculated by assuming the reversal potentials for $I_{Ca,T}$ and $I_{Ca,L}$ to be the zero-current potentials measured in the *I-V* relationships. The smooth curves through the data points represent a least-squares fit with a Boltzmann equation, yielding $V_{1/2}$ and k for $I_{Ca,T}$ and $I_{Ca,L}$ (see Table 2). *$P < 0.05$ and **$P < 0.01$ compared with control.

estly but significantly decreased spontaneous firing rate as well as DDR, suggesting that $I_{Ca,T}$ contributes at least partly to diastolic depolarization and spontaneous activity of SA node cells in guinea-pig heart.

Figure 10C illustrates superimposed action potentials recorded before and during exposure to increasing concentrations of nifedipine (1 nM–1 μM) in a cumulative manner. Spontaneous firing rate and DDR were not significantly affected by nifedipine at 1 and 10 nM but were significantly reduced by nifedipine at 100 nM. In most of cells examined (six out of eight cells), spontaneous firing of SA node cells was stopped by 1 μM nifedipine, which is consistent with previous observation in the centre of SA node in a rabbit heart (Kodama *et al.*, 1997). It should be noted that nifedipine significantly decreased the max dV·dt⁻¹ at all concentrations tested (control, 7.4 ± 1.8 V·s⁻¹; nifedipine, 1 nM, 4.9 ± 1.4 V·s⁻¹; 10 nM, 3.9 ± 1.5 V·s⁻¹; 100 nM, 2.1 ± 0.7 V·s⁻¹; $n = 8$, $N = 4$).

Suppressive effects of sevoflurane on I_{Ks} in SA node cells

Figure 11 shows representative experiments examining the effect of sevoflurane on I_{Ks} in guinea-pig SA node cells. As demonstrated in lower panel of Figure 11A, 0.44 mM sevoflurane rapidly and reversibly inhibited I_{Ks}, repetitively (every 15 s) activated by 4 s depolarizing steps to +40 mV applied from a holding potential of −50 mV. In another set of experiments, I_{Ks} was recorded at test potentials of −40 to +40 mV, before and during exposure to 0.44 mM sevoflurane, and after its washout (Figure 11A, upper panel). The inhibitory effect of sevoflurane on I_{Ks} was assessed by measuring the amplitude of the tail current, which reflects the degree of I_{Ks} activation at the preceding depolarizing test potential. Sevoflurane reversibly reduced the amplitude of I_{Ks} tail current by 37.1 ± 4.2% ($n = 6$, $N = 3$), measured at a test potential of +40 mV (Figure 11B,C). Voltage dependence of I_{Ks} activation was evaluated by fitting the amplitude of tail current with a Boltzmann equation (Figure 11B). There were no significant differences in values for $V_{1/2}$ and k recorded before and during exposure to sevoflurane, and after its washout (Table 2), indicating that sevoflurane had a little effect on the voltage dependence of I_{Ks} activation. The time course of I_{Ks} deactivation was analysed by fitting the tail current with two exponential functions, yielding the fast and slow time constants (τ_f and τ_s respectively; Figure 11D). These values were not significantly altered by sevoflurane, indicating that I_{Ks} deac-

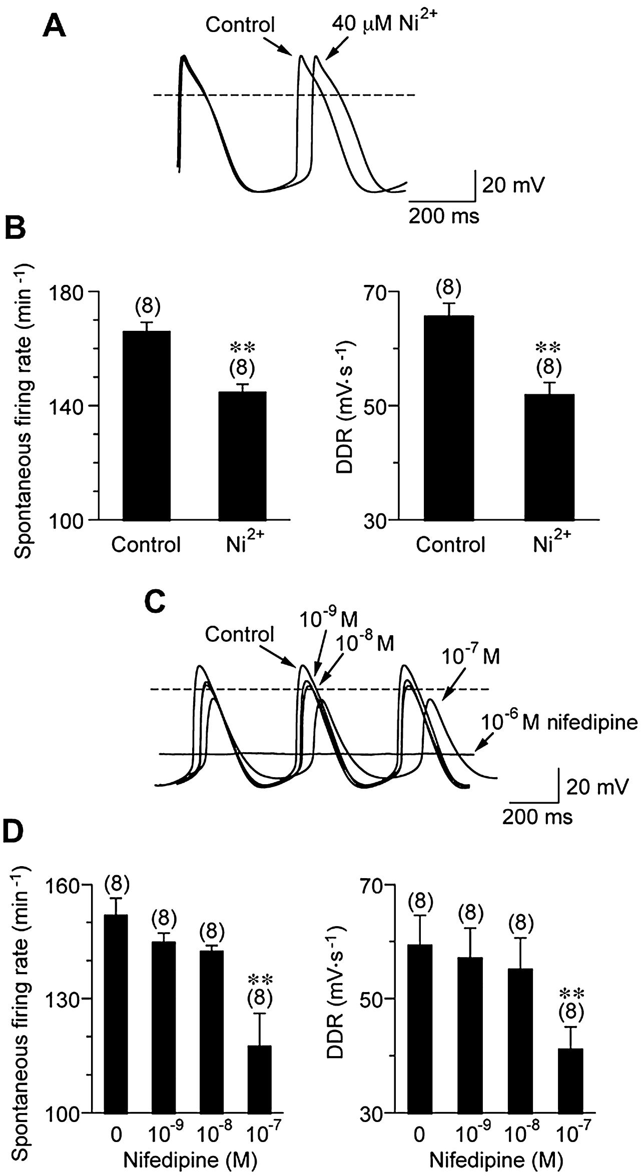

Figure 10

Effects of $NiCl_2$ and nifedipine on spontaneous activity of guinea-pig SA node cells. (A) Superimposed action potentials recorded before and 5 min after exposure to 40 μM $NiCl_2$. (B) Summarized data for spontaneous firing rate (left panel) and DDR (right) recorded before (control) and 5 min after exposure to 40 μM $NiCl_2$. (C) Superimposed action potentials recorded before (control) and during exposure to increasing concentrations of nifedipine (1 nM–1 μM), in a cumulative way, with each concentration applied for 6–8 min. (D) Summarized data for spontaneous firing rate (left panel) and DDR (right) recorded before and 6–8 min after exposure to nifedipine. The number of cells is shown in parenthesis, obtained from 3 ($NiCl_2$) and 4 (nifedipine) cell isolations. ***P* < 0.01 compared with control.

tivation (transition from open to closed state) was not affected by sevoflurane. We also examined the effects of 0.71 mM sevoflurane on I_{Ks} using the voltage-clamp protocols similar to those of Figure 11 and found that 0.71 mM sevoflurane inhibited I_{Ks} by 53.6 ± 5.5% (n = 4, N = 2) without significantly affecting the voltage dependence of current activation (Table 2) and time course of deactivation (data not shown).

Effect of sevoflurane on heart rate ex vivo in Langendorff mode and in vivo in sevoflurane-anaesthetized guinea-pigs

We next examined the effects of sevoflurane on heart rate *ex vivo* in isolated Langendorff-perfused guinea-pig hearts and *in vivo* in sevoflurane-anaesthetized guinea-pigs (Figure 12). There were no significant effects of sevoflurane on heart rate when guinea-pigs were anaesthetized by sevoflurane inhalation at concentrations of 1, 3 and 5%. In contrast, heart rate in isolated Langendorff-perfused guinea-pig hearts was significantly decreased by administration of sevoflurane at concentrations of 0.12, 0.44 and 0.71 mM.

Computer simulation of sevoflurane effect on spontaneous action potentials

We finally conducted a computer simulation study to examine the impact of changes in individual currents (I_f, $I_{Ca,T}$, $I_{Ca,L}$ and I_{Ks}) on the negative chronotropic action of sevoflurane using the SA node cell model of Kurata *et al.* (2002). Our voltage-clamp experiments found that sevoflurane at 0.44 mM reduced the conductances for I_f, $I_{Ca,T}$, $I_{Ca,L}$ and I_{Ks} by 14.4, 31.3, 30.3 and 37.1%, respectively, which were used for the present model calculation. The firing frequency of spontaneous action potentials was decreased by simulating these inhibitory effects of sevoflurane on I_f, $I_{Ca,T}$, $I_{Ca,L}$ and I_{Ks} in the Kurata SA node cell model (Figure 13A–E). It is interesting to note that inward I_{NCX} is appreciably reduced during diastolic depolarization phase in the simulation of sevoflurane effect (Figure 13F). Figure 13G compares the percent decreases in firing rate, DDR, MDP, APA and max $dV{\cdot}dt^{-1}$ in spontaneous action potentials by sevoflurane (0.44 mM) obtained experimentally in SA node cells and in the computer simulations. Although there are some differences in the degree of percent changes in these action potential parameters between experimental and simulation studies, the Kurata SA node cell model was able to reproduce, reasonably, the experimental data for the inhibitory effect of sevoflurane on spontaneous activity of SA node cells (Figures 1 and 2).

To estimate the effects of changes in individual currents (I_f, $I_{Ca,T}$, $I_{Ca,L}$ and I_{Ks}) on the negative chronotropy associated with sevoflurane (0.44 mM), the percent decrease in firing rate was calculated by reducing the conductance for each current by the degree observed in the voltage-clamp experiments. This computer simulation analysis indicates that the negative chronotropy induced by sevoflurane is comprised of inhibition of three membrane currents, in the order of $I_{Ca,T} \geq I_{Ca,L} > I_f$ with little contribution from I_{Ks}. Because relatively low (0.0259 $nS{\cdot}pF^{-1}$) conductance of I_{Ks} is incorporated in the Kurata SA node model, reducing I_{Ks} produced only a minimal effect on the electrical activity of SA node cells. It is generally accepted that model calculations have some limitations and may not fully reproduce all of the experimental phenomena (Kurata *et al.*, 2002).

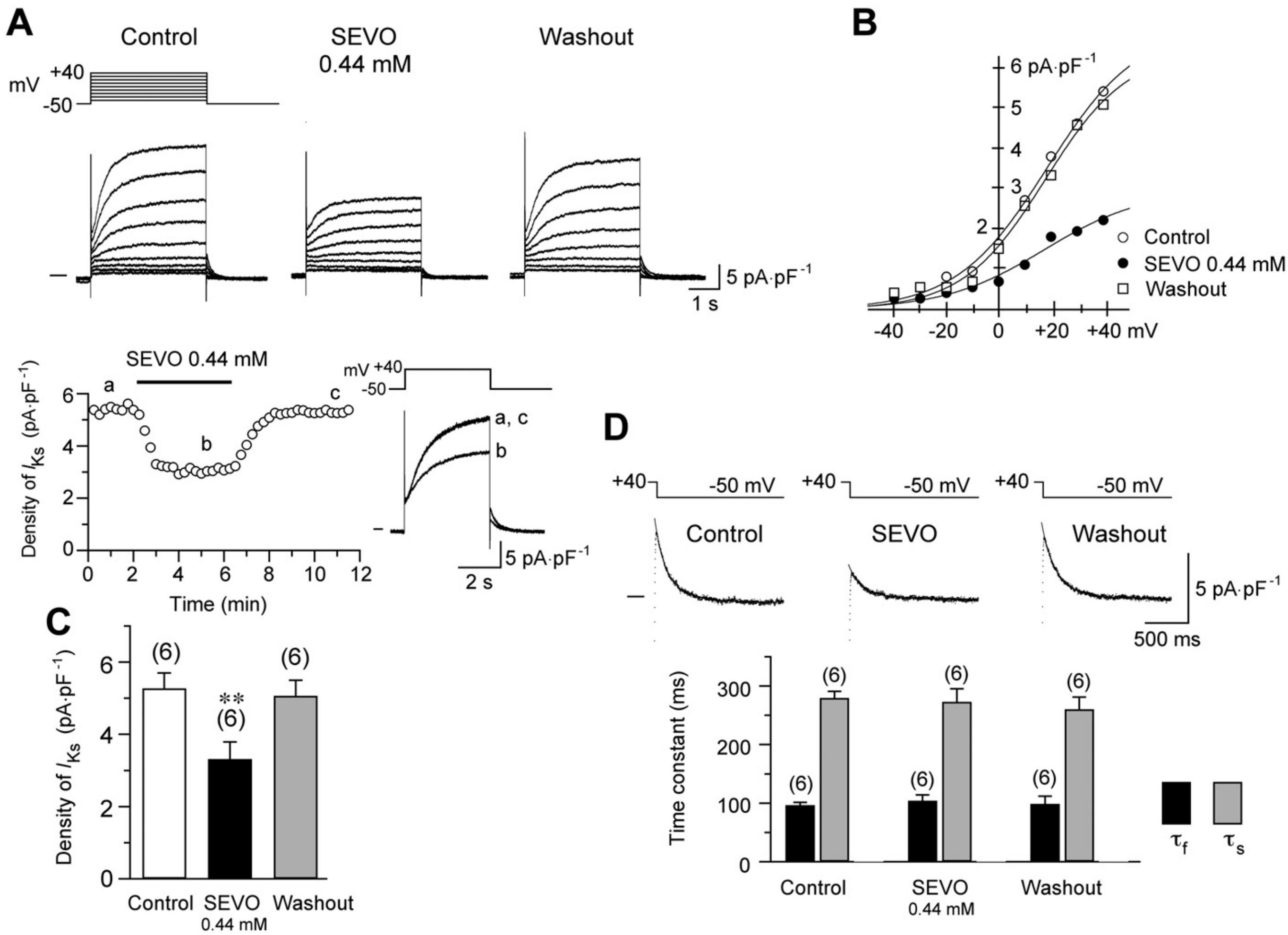

Figure 11

Suppressive effect of sevoflurane (SEVO) on I_{Ks}. (A) Upper panel shows voltage-clamp protocol and superimposed current traces of I_{Ks}, activated during 4 s depolarizing voltage steps applied from a holding potential of –50 mV to test potentials of –40 to +40 mV, before and 3 min after exposure to 0.44 mM SEVO, and 5 min after washout. Lower panel shows time course of changes in the amplitude of I_{Ks} tail current during exposure to 0.44 mM sevoflurane. I_{Ks} was repetitively (every 15 s) activated by 4 s depolarizing steps to +40 mV from a holding potential of –50 mV. Original current traces recorded at time points indicated by characters are also shown (a, b and c). The experiments in upper and lower panels were obtained from different cells. (B) *I-V* relationships of I_{Ks} tail currents elicited upon return to a holding potential of –50 mV from data shown in upper panel of (A), fitted with a Boltzmann equation (smooth curves), yielding $V_{1/2}$ and *k* (see Table 2). Note that the values for $V_{1/2}$ and *k* after washout ($V_{1/2}$, 17.9 ± 1.1 mV; *k*, 14.1 ± 0.7 mV, $n = 6$, $N = 3$) are not significantly different from those recorded before and during exposure to sevoflurane (see Table 2). (C) Amplitudes of I_{Ks} tail currents elicited following depolarizing step to +40 mV, before and during exposure to 0.44 mM sevoflurane, and after washout ($n = 6$, $N = 3$). **$P < 0.01$ compared with either control or washout (no significant difference between control and washout). (D) Summarized data for time constants of fast and slow components of I_{Ks} tail currents (τ_f and τ_s, respectively) in each condition ($n = 6$, $N = 3$). The inset shows the original current traces (dotted points) fitted with two exponential functions (continuous curve).

Discussion

One minimum alveolar concentration (MAC) of sevoflurane is approximately 2% in humans (Frink *et al*., 1992), and in the clinical settings, sevoflurane is usually administered at concentrations of above 0.8 MAC to maintain anaesthesia and to prevent awareness during anaesthesia (Ghoneim, 2000; Avidan *et al*., 2008). It has been reported that the blood concentration of sevoflurane ranges between approximately 0.29 and 0.65 mM in patients during inhalation of sevoflurane at concentrations of ≥2% (Frink *et al*., 1992; Matsuse *et al*., 2011). The present experiments examined the electrophysiological effects of sevoflurane at concentrations ranging between 0.12 and 0.71 mM, which is relevant to the clinically used concentrations. We found for the first time that sevoflurane in this range produces a concentration-dependent inhibitory effect on SA node automaticity (Figures 1 and 2).

The diastolic depolarization of SA node action potentials is important not only for generating the spontaneous activity but also for regulating the firing frequency (DiFrancesco, 1993; Honjo *et al*., 1996; Dobrzynski *et al*., 2007; Mangoni and Nargeot, 2008; Verkerk *et al*., 2009; Baruscotti *et al*., 2010). Stimulation of β-adrenergic and muscarinic receptors, respectively, accelerates and decelerates the spontaneous

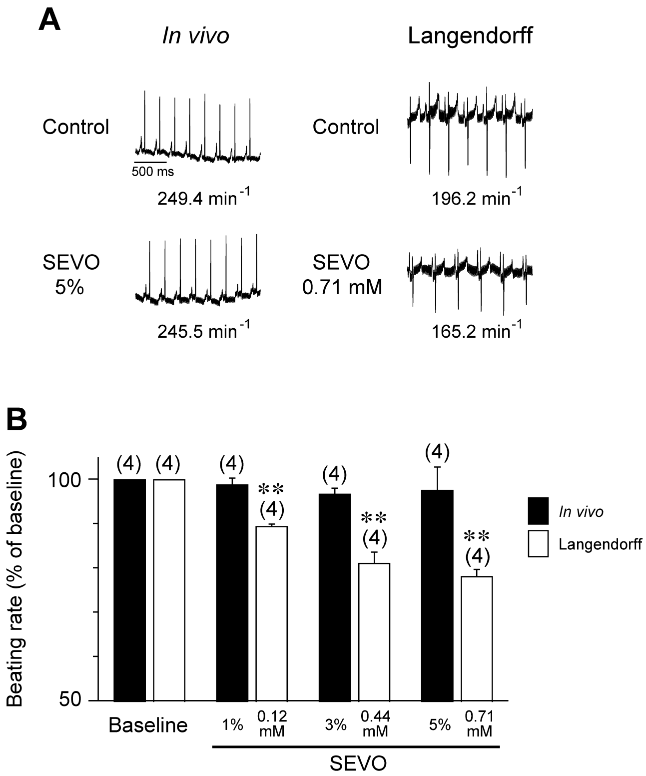

Figure 12

Effects of sevoflurane (SEVO) on heart rate *ex vivo* in isolated perfused guinea-pig hearts and *in vivo* in sevoflurane-anaesthetized guinea-pigs. (A) Representative ECG recordings before and during 5% sevoflurane inhalation *in vivo* (left panels) and those before and during administration of 0.71 mM sevoflurane in isolated Langendorff-perfused heart (right panels). (B) Heart rate *in vivo* in sevoflurane-anaesthetized guinea-pigs at concentrations of 1, 3 and 5% ($N = 4$) and *ex vivo* in Langendorff-perfused guinea-pig hearts during administration of sevoflurane at concentrations of 0.12, 0.44 and 0.71 mM ($N = 4$). Data are expressed as normalized values with reference to their respective baseline values (248.0 ± 13.9 min^{-1} in *in vivo* conditions and 205.5 ± 6.5 min^{-1} in Langendorff perfusion mode) recorded before administration of sevoflurane. $^{**}P < 0.01$ compared with baseline.

firing of SA node cells mainly by modulating DDR (DiFrancesco, 1993). The present experiments revealed that sevoflurane reduced DDR and spontaneous firing frequency in a qualitatively similar concentration-dependent manner (Figure 2). This observation strongly suggests that sevoflurane decelerated spontaneous activity of SA node cells primarily by slowing the diastolic depolarization.

I_f is activated during the repolarization phase of SA node cells and thereby produces an inward current that helps to trigger the diastolic depolarization (DiFrancesco, 1991; 1993; BoSmith *et al*., 1993; Mangoni and Nargeot, 2001; 2008; Dobrzynski *et al*., 2007; Verkerk *et al*., 2007; 2009; Baruscotti *et al*., 2010; Gao *et al*., 2010). The present experiment using the I_f blocker zatebradine also supports the proposal that I_f contributes to SA node automaticity in guinea-pig heart (Figure 3). Sevoflurane concentration-dependently inhibited I_f with an IC_{50} of 0.37 mM (Figure 5C), which is close to the inhibitory action of sevoflurane on firing frequency (0.34 mM) and DDR (0.34 mM) in spontaneous action potentials (Figure 2). These observations suggest that the inhibitory action of sevoflurane on I_f is at least partly related to the reduction of DDR associated with decrease in spontaneous activity of SA node cells.

Other ionic mechanisms also mediate the diastolic depolarization of SA node action potentials. Our experiments revealed that $I_{Ca,T}$ is present (Figures 8 and 9) and plays a role in diastolic depolarization and spontaneous activity in SA node cells of guinea-pig (Figure 10A,B), consistent with the observation in rabbit SA node cells (Hagiwara *et al*., 1988). It is therefore probable that the inhibitory action on $I_{Ca,T}$ (Figures 8 and 9) contributed to the negative chronotropic action of sevoflurane. On the other hand, evidence has been presented to indicate that $I_{Ca,L}$ also mediates the diastolic depolarization in rabbit SA node cells (Verheijck *et al*., 1999). The present results showed that nifedipine stopped the spontaneous activity at a high concentration (1 μM) and moderately decreased the diastolic depolarization associated with reduction of firing frequency at an intermediate concentration (100 nM; Figure 10C,D). These observations suggest that $I_{Ca,L}$ contributes not only to the rapid depolarization phase but also to the slow diastolic depolarization of SA node action potentials.

However, pharmacological blockade of $I_{Ca,L}$ during the action potentials in current-clamp experiments could affect the activities of other ionic channels and transporters responsible for the diastolic depolarization as well as for the repolarization phase. For example, reduced Ca^{2+} influx through $I_{Ca,L}$ could decrease the activation of inward I_{NCX} by Ca^{2+} release from the sarcoplasmic reticulum (Mangoni *et al*., 2006), which has been shown to play an essential role in SA node automaticity (Ca^{2+} clock mechanism, Bogdanov *et al*., 2006). The present computer simulations using the Kurata model also show that a simulated reduction of $I_{Ca,L}$ results in a discernible decrease in inward I_{NCX} during diastolic depolarization (Figure 13). Thus, the inhibition of $I_{Ca,L}$ by sevoflurane is likely to contribute to the negative chronotropic action either directly or through a mechanism involving reduced I_{NCX}. Further studies are required to examine the direct effect of sevoflurane on I_{NCX} and/or Ca^{2+} release from the sarcoplasmic reticulum in SA node cells.

I_{Ks} plays an important role in repolarization of spontaneous action potentials in guinea-pig SA node cells (Matsuura *et al*., 2002). The present current-clamp experiments showed that MDP was gradually depolarized by increasing the concentrations of sevoflurane (Table 1), which may be consistent with the inhibitory action of sevoflurane on I_{Ks} (Figure 11). On the other hand, sevoflurane did not significantly affect APD_{50} and APD_{90} (Table 1). Because reductions of I_{Ks} and $I_{Ca,L}$ have opposite effects on action potential duration (APD), dual inhibition of I_{Ks} and $I_{Ca,L}$ in the presence of sevoflurane is likely to mask their opposite actions on APD. It should be added that the inhibition of I_{Ks} may contribute to the negative chronotropic action of sevoflurane by depolarizing MDP, and thereby affecting the activities of other ionic currents responsible for the diastolic depolarization, such as I_f.

It remains unclear whether the inhibitory action of sevoflurane on I_f, $I_{Ca,T}$, $I_{Ca,L}$ and I_{Ks} arises from direct binding to the channel proteins or is mediated indirectly through the interaction with the modulatory proteins and/or lipid membranes

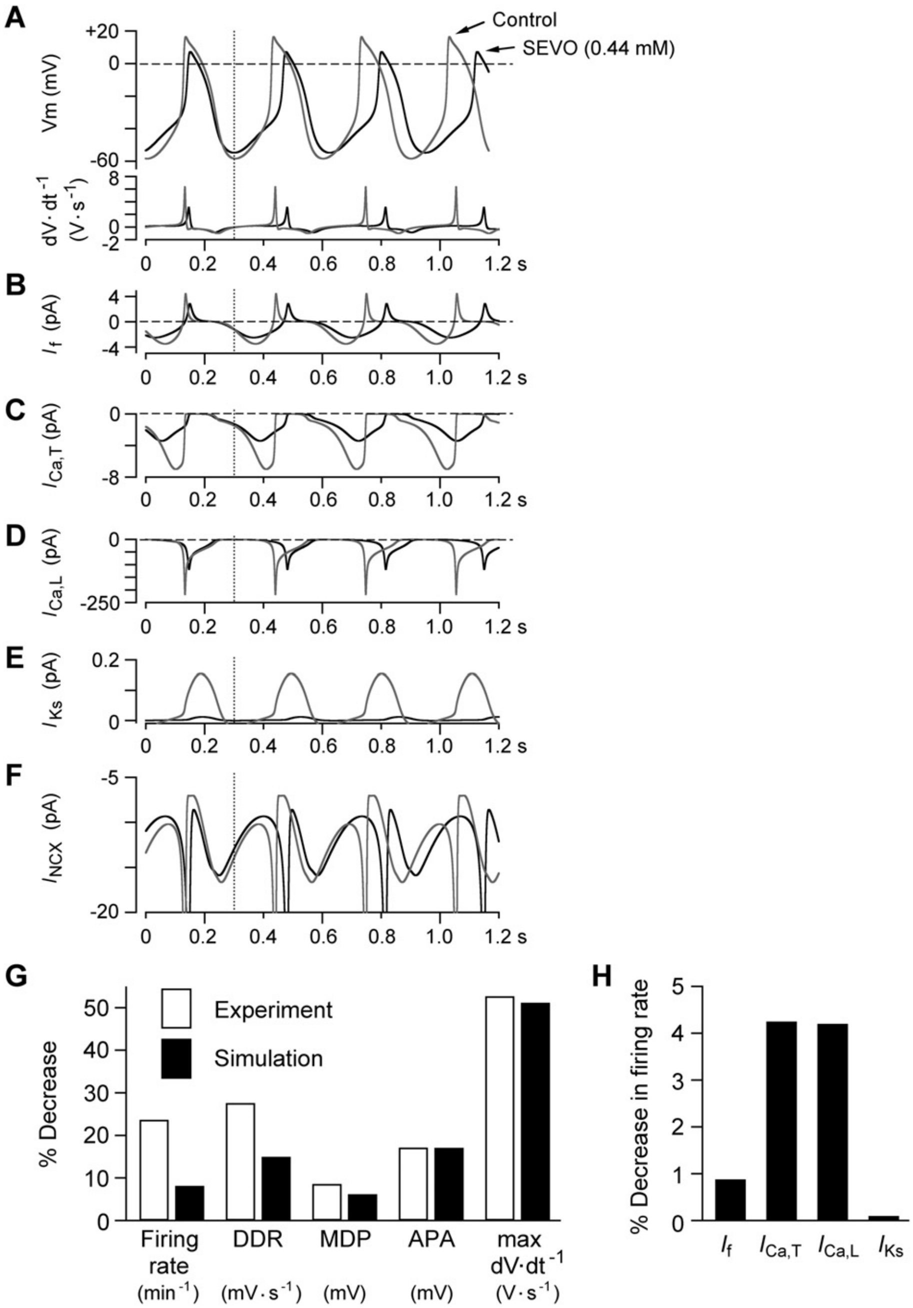

Figure 13

Negative chronotropic effects of sevoflurane (SEVO) on spontaneous activity of SA node cell model. (A) Spontaneous action potentials and their first derivatives ($dV{\cdot}dt^{-1}$) in control and in the presence of 0.44 mM sevoflurane in the Kurata SA node model simulated by decreasing the conductance for I_f, $I_{Ca,T}$, $I_{Ca,L}$ and I_{Ks}. The MDP of the first action potentials in control and in the presence of sevoflurane is superimposed and denoted by vertical dotted lines. (B–E) Changes in I_f, $I_{Ca,T}$, $I_{Ca,L}$ and I_{Ks} during spontaneous action potentials in SA node cell model, obtained by decreasing the conductance for each current by the same degree as in voltage-clamp experiments with 0.44 mM sevoflurane (14.4% reduction in I_f, 31.3% reduction in $I_{Ca,T}$, 30.3% reduction in $I_{Ca,L}$ or 37.1% reduction in I_{Ks}). (F) Simulated changes in the amplitude of I_{NCX} during spontaneous action potentials in the absence and presence of sevoflurane. The peak of I_{NCX} is off the scale. (G) Comparison of percent decrease in firing rate, DDR, MDP, APA and max $dV{\cdot}dt^{-1}$ in spontaneous action potentials by sevoflurane (0.44 mM) in current-clamp experiments and simulation studies. The experimental data were the same as those shown in Figure 2 and Table 1. (H) Percent decrease in spontaneous firing rate when each conductance for I_f, $I_{Ca,T}$, $I_{Ca,L}$ or I_{Ks} was individually decreased in the SA node cell model by the degree of experimental results with 0.44 mM sevoflurane. It should be noted that the present model calculation was conducted only by simulating the reduction of conductances for these currents without changing other electrophysiological parameters.

in which channel proteins are embedded. It should, however, be noted that the inhibitory actions of sevoflurane on all of these ionic currents are rapidly and almost completely reversed within 1–2 min after washout, which appears to be a favourable property for clinical use. Other studies are needed to elucidate the cellular and/or molecular mechanisms mediating the inhibitory action of sevoflurane on these ion channels.

A clinical electrophysiological study did not detect any appreciable effect of sevoflurane on heart rate and SA node function in patients with Wolff–Parkinson–White syndrome (Sharpe *et al.*, 1999). Furthermore, most of clinical investigations showed that sevoflurane inhalation does not profoundly alter heart rate from the awake (baseline) value (Holaday and Smith, 1981; Frink *et al.*, 1992; Lerman *et al.*, 1994; Malan *et al.*, 1995; Ebert *et al.*, 1995a,b; Smith *et al.*, 1996). We also found that there were no significant alterations in heart rate *in vivo* in sevoflurane-anaesthetized guinea-pigs (Figure 12), which appears to be similar to those reported in these earlier clinical observations. Direct negative chronotropic effects of sevoflurane observed in SA node cells (Figures 1 and 2) and isolated Langendorff-perfused hearts (Figure 12) are thus masked in *in vivo* conditions, where the autonomic nervous system functions to regulate heart rate. In addition, there is clinical evidence that sevoflurane affects both sympathetic and parasympathetic nerve activities and thereby modulates the heart rate (Paisansathan *et al.*, 2007). Accordingly, it may be difficult to explain changes in heart rate during sevoflurane anaesthesia only by its direct electrophysiological action on the SA node. However, it is important to understand that sevoflurane itself has a direct inhibitory effect on SA node automaticity via affecting ion channel functions such as I_f, $I_{Ca,T}$ and $I_{Ca,L}$. It is therefore expected that negative chronotropic action of sevoflurane could be exaggerated in patients treated with pharmacological blockers of these ion channels or with compromised channel functions associated with gene mutations.

In conclusion, we have provided the first detailed electrophysiological evidence that clinical relevant concentrations of sevoflurane have a direct negative chronotropic effect on SA node automaticity, which may be at least partly due to its inhibitory action on I_f, $I_{Ca,T}$ and $I_{Ca,L}$. These findings may constitute an important electrophysiological basis of the mechanisms underlying the various changes in heart rate observed during sevoflurane anaesthesia in clinical settings.

Acknowledgements

The authors gratefully acknowledge the advice and help of Dr. Yukiko Himeno (Kyoto University, Japan) for the computer simulation studies. This study was supported by Grant-in-Aid for Scientific Research from Ministry of Education, Culture, Sports, Science and Technology-Japan (No. 22791426 to AK) and from Japan Society for the Promotion of Science (No. 21591971 to HK).

Conflicts of interest

None.

References

Alexander SPH, Mathie A, Peters JA (2011). Guide to receptors and channels (GRAC), 5th edn. Br J Pharmacol 164 (Suppl. 1): S1–S324.

Avidan MS, Zhang L, Burnside BA, Finkel KJ, Searleman AC, Selvidge JA *et al.* (2008). Anesthesia awareness and the bispectral index. N Engl J Med 358: 1097–1108.

Baruscotti M, Bucchi A, Difrancesco D (2005). Physiology and pharmacology of the cardiac pacemaker ('funny') current. Pharmacol Ther 107: 59–79.

Baruscotti M, Barbuti A, Bucchi A (2010). The cardiac pacemaker current. J Mol Cell Cardiol 48: 55–64.

Belardinelli L, Giles WR, West A (1988). Ionic mechanisms of adenosine actions in pacemaker cells from rabbit heart. J Physiol 405: 615–633.

Bénitah JP, Gomez AM, Bailly P, Da Ponte JP, Berson G, Delgado C *et al.* (1993). Heterogeneity of the early outward current in ventricular cells isolated from normal and hypertrophied rat hearts. J Physiol 469: 111–138.

Bernard JM, Wouters PF, Doursout MF, Florence B, Chelly JE, Merin RG (1990). Effects of sevoflurane and isoflurane on cardiac and coronary dynamics in chronically instrumented dogs. Anesthesiology 72: 659–662.

Bogdanov KY, Maltsev VA, Vinogradova TM, Lyashkov AE, Spurgeon HA, Stern MD *et al.* (2006). Membrane potential fluctuations resulting from submembrane Ca^{2+} releases in rabbit sinoatrial nodal cells impart an exponential phase to the late diastolic depolarization that controls their chronotropic state. Circ Res 99: 979–987.

BoSmith RE, Briggs I, Sturgess NC (1993). Inhibitory actions of ZENECA ZD7288 on whole-cell hyperpolarization activated inward current (I_f) in guinea-pig dissociated sinoatrial node cells. Br J Pharmacol 110: 343–349.

Bosnjak ZJ, Kampine JP (1983). Effects of halothane, enflurane, and isoflurane on the SA node. Anesthesiology 58: 314–321.

DiFrancesco D (1991). The contribution of the 'pacemaker' current (i_f) to generation of spontaneous activity in rabbit sino-atrial node myocytes. J Physiol 434: 23–40.

DiFrancesco D (1993). Pacemaker mechanisms in cardiac tissue. Annu Rev Physiol 55: 455–472.

Dobrzynski H, Boyett MR, Anderson RH (2007). New insights into pacemaker activity. Promoting understanding of sick sinus syndrome. Circulation 115: 1921–1932.

Ebert TJ, Harkin CP, Muzi M (1995a). Cardiovascular responses to sevoflurane: a review. Anesth Analg 81 (Suppl.): S11–S22.

Ebert TJ, Muzi M, Lopatka CW (1995b). Neurocirculatory responses to sevoflurane in humans. A comparison to desflurane. Anesthesiology 83: 88–95.

Fabiato A, Fabiato F (1979). Calculator programs for computing the composition of the solutions containing multiple metals and ligands used for experiments in skinned muscle cells. J Physiol (Paris) 75: 463–505.

Frink EJ Jr, Malan TP, Atlas M, Dominguez LM, DiNardo JA, Brown BR Jr (1992). Clinical comparison of sevoflurane and isoflurane in healthy patients. Anesth Analg 74: 241–245.

Gao Z, Chen B, Joiner ML, Wu Y, Guan X, Koval OM *et al*. (2010). I_f and SR Ca^{2+} release both contribute to pacemaker activity in canine sinoatrial node cells. J Mol Cell Cardiol 49: 33–40.

Ghoneim MM (2000). Awareness during anesthesia. Anesthesiology 92: 597–602.

van Ginneken ACG, Giles W (1991). Voltage clamp measurements of the hyperpolarization-activated inward current I_f in single cells from rabbit sino-atrial node. J Physiol 434: 57–83.

Goethals M, Raes A, van Bogaert P-P (1993). Use-dependent block of the pacemaker current I_f in rabbit sinoatrial node cells by zatebradine (UL-FS 49). On the mode of action of sinus node inhibitors. Circulation 88: 2389–2401.

Guo J, Mitsuiye T, Noma A (1997). The sustained inward current in sino-atrial node cells of guinea-pig heart. Pflügers Arch 433: 390–396.

Hagiwara N, Irisawa H, Kameyama M (1988). Contribution of two types of calcium currents to the pacemaker potentials of rabbit sino-atrial node cells. J Physiol 395: 233–253.

Hagiwara N, Irisawa H, Kasanuki H, Hosoda S (1992). Background current in sino-atrial node cells of the rabbit heart. J Physiol 448: 53–72.

Hamill OP, Marty A, Neher E, Sakmann B, Sigworth FJ (1981). Improved patch-clamp techniques for high-resolution current recording from cells and cell-free membrane patches. Pflügers Arch 391: 85–100.

Holaday DA, Smith FR (1981). Clinical characteristics and biotransformation of sevoflurane in healthy human volunteers. Anesthesiology 54: 100–106.

Honjo H, Boyett MR, Kodama I, Toyama J (1996). Correlation between electrical activity and the size of rabbit sino-atrial node cells. J Physiol 496: 795–808.

Horn R, Marty A (1988). Muscarinic activation of ionic currents measured by a new whole-cell recording method. J Gen Physiol 92: 145–159.

Isenberg G, Klöckner U (1982). Calcium tolerant ventricular myocytes prepared by preincubation in a 'KB medium'. Pflügers Arch 395: 6–18.

Kodama I, Nikmaram MR, Boyett MR, Suzuki R, Honjo H, Owen JM (1997). Regional differences in the role of the Ca^{2+} and Na^+ currents in pacemaker activity in the sinoatrial node. Am J Physiol 272: H2793–H2806.

Kojima A, Kitagawa H, Omatsu-Kanbe M, Matsuura H, Nosaka S (2011). Sevoflurane protects ventricular myocytes from Ca^{2+} paradox-mediated Ca^{2+} overload by blocking the activation of transient receptor potential canonical channels. Anesthesiology 115: 509–522.

Kurata Y, Hisatome I, Imanishi S, Shibamoto T (2002). Dynamical description of sinoatrial node pacemaking: improved mathematical model for primary pacemaker cell. Am J Physiol 283: H2074–H2101.

Lerman J, Sikich N, Kleinman S, Yentis S (1994). The pharmacology of sevoflurane in infants and children. Anesthesiology 80: 814–824.

Lipscombe D (2002). L-type calcium channels. Highs and new lows. Circ Res 90: 933–935.

Malan TP Jr, DiNardo JA, Isner RJ, Frink EJ Jr, Goldberg M, Fenster PE *et al*. (1995). Cardiovascular effects of sevoflurane compared with those of isoflurane in volunteers. Anesthesiology 83: 918–928.

Mangoni ME, Nargeot J (2001). Properties of the hyperpolarization-activated current (I_f) in isolated mouse sino-atrial cells. Cardiovasc Res 52: 51–64.

Mangoni ME, Nargeot J (2008). Genesis and regulation of the heart automaticity. Physiol Rev 88: 919–982.

Mangoni ME, Couette B, Bourinet E, Platzer J, Reimer D, Striessnig J *et al*. (2003). Functional role of L-type $Ca_v1.3$ Ca^{2+} channels in cardiac pacemaker activity. Proc Natl Acad Sci U S A 100: 5543–5548.

Mangoni ME, Couette B, Marger L, Bourinet E, Striessnig J, Nargeot J (2006). Voltage-dependent calcium channels and cardiac pacemaker activity: from ionic currents to genes. Prog Biophys Mol Biol 90: 38–63.

Manohar M, Parks CM (1984). Porcine systemic and regional organ blood flow during 1.0 and 1.5 minimum alveolar concentrations of sevoflurane anesthesia without and with 50% nitrous oxide. J Pharmacol Exp Ther 231: 640–648.

Matsuse S, Hara Y, Ohkura T (2011). The possible influence of pulmonary arterio-venous shunt and hypoxic pulmonary vasoconstriction on arterial sevoflurane concentration during one-lung ventilation. Anesth Analg 112: 345–348.

Matsuura H, Ehara T, Ding WG, Omatsu-Kanbe M, Isono T (2002). Rapidly and slowly activating components of delayed rectifier K^+ current in guinea-pig sino-atrial node pacemaker cells. J Physiol 540: 815–830.

McGrath JC, Drummond GB, McLachlan EM, Kilkenny C, Wainwright CL (2010). Guidelines for reporting experiments involving animals: the ARRIVE guidelines. Br J Pharmacol. 160: 1573–1576.

Milanesi R, Baruscotti M, Gnecchi-Ruscone T, DiFrancesco D (2006). Familial sinus bradycardia associated with a mutation in the cardiac pacemaker channel. N Engl J Med 354: 151–157.

Nof E, Luria D, Brass D, Marek D, Lahat H, Reznik-Wolf H *et al*. (2007). Point mutation in the HCN4 cardiac ion channel pore affecting synthesis, trafficking, and functional expression is associated with familial asymptomatic sinus bradycardia. Circulation 116: 463–470.

Ono K, Shibata S, Iijima T (2000). Properties of the delayed rectifier potassium current in porcine sino-atrial node cells. J Physiol 524: 51–62.

Paisansathan C, Lee M, Hoffman WE, Wheeler P (2007). Sevoflurane anesthesia decreases cardiac vagal activity and heart rate variability. Clin Auton Res 17: 370–374.

Rigg L, Mattick PAD, Heath BM, Terrar DA (2003). Modulation of the hyperpolarization-activated current (I_f) by calcium and calmodulin in the guinea-pig sino-atrial node. Cardiovasc Res 57: 497–504.

Sarai N, Matsuoka S, Noma A (2006). *simBio*: a Java package for the development of detailed cell models. Prog Biophys Mol Biol 90: 360–377.

Schulze-Bahr E, Neu A, Friederich P, Kaupp UB, Breithardt G, Pongs O *et al*. (2003). Pacemaker channel dysfunction in a patient with sinus node disease. J Clin Invest 111: 1537–1545.

Sharpe MD, Cuillerier DJ, Lee JK, Basta M, Krahn AD, Klein GJ *et al*. (1999). Sevoflurane has no effect on sinoatrial node function or on normal atrioventricular and accessory pathway conduction in Wolff-Parkinson-White syndrome during alfentanil/midazolam anesthesia. Anesthesiology 90: 60–65.

Shi W, Wymore R, Yu H, Wu J, Wymore RT, Pan Z *et al*. (1999). Distribution and prevalence of hyperpolarization-activated cation channel (HCN) mRNA expression in cardiac tissues. Circ Res 85: e1–e6.

Smith I, Nathanson M, White PF (1996). Sevoflurane – a long-awaited volatile anaesthetic. Br J Anaesth 76: 435–445.

Tellez JO, Dobrzynski H, Greener ID, Graham GM, Laing E, Honjo H *et al*. (2006). Differential expression of ion channel transcripts in atrial muscle and sinoatrial node in rabbit. Circ Res 99: 1384–1393.

Thollon C, Bedut S, Villeneuve N, Cogé F, Piffard L, Guillaumin J-P *et al*. (2007). Use-dependent inhibition of hHCN4 by ivabradine and relationship with reduction in pacemaker activity. Br J Pharmacol 150: 37–46.

Tsien RY, Rink TJ (1980). Neutral carrier ion-selective microelectrodes for measurement of intracellular free calcium. Biochim Biophys Acta 599: 623–638.

Ueda K, Nakamura K, Hayashi T, Inagaki N, Takahashi M, Arimura T *et al*. (2004). Functional characterization of a trafficking-defective HCN4 mutation, D553N, associated with cardiac arrhythmia. J Biol Chem 279: 27194–27198.

Verheijck EE, van Ginneken ACG, Bourier J, Bouman LN (1995). Effects of delayed rectifier current blockade by E-4031 on impulse generation in single sinoatrial nodal myocytes of the rabbit. Circ Res 76: 607–615.

Verheijck EE, van Ginneken AC, Wilders R, Bouman LN (1999). Contribution of L-type Ca^{2+} current to electrical activity in sinoatrial nodal myocytes of rabbits. Am J Physiol 276: H1064–H1077.

Verkerk AO, Wilders R, van Borren MM, Peters RJ, Broekhuis E, Lam K *et al*. (2007). Pacemaker current (I_f) in the human sinoatrial node. Eur Heart J 28: 2472–2478.

Verkerk AO, van Ginneken ACG, Wilders R (2009). Pacemaker activity of the human sinoatrial node: role of the hyperpolarization-activated current, I_f. Int J Cardiol 132: 318–336.